Star Clusters:
From Infancy to Teenagehood
Max-Plank Haus, Heidelberg, Germany, 8 – 12 August 2016
Genevieve Parmentier

- **Session 1 Star Clusters in the Making**
- **Session 2 Multiple Stellar Populations in Clusters**
- **Session 3 Cluster Dissolution**

A revised moving cluster distance to the Pleiades open cluster

P.A.B. Galli, E. Moraux, H. Bouy et al.

arXiv:1610.05641

120 ± 1.9 pc (van Leeuwen 2007, HIPPARCOS)

136.2 ± 1.2 pc (Melis+ 2014, VLBI)

DANCE – proper motions

APOGEE - Vr

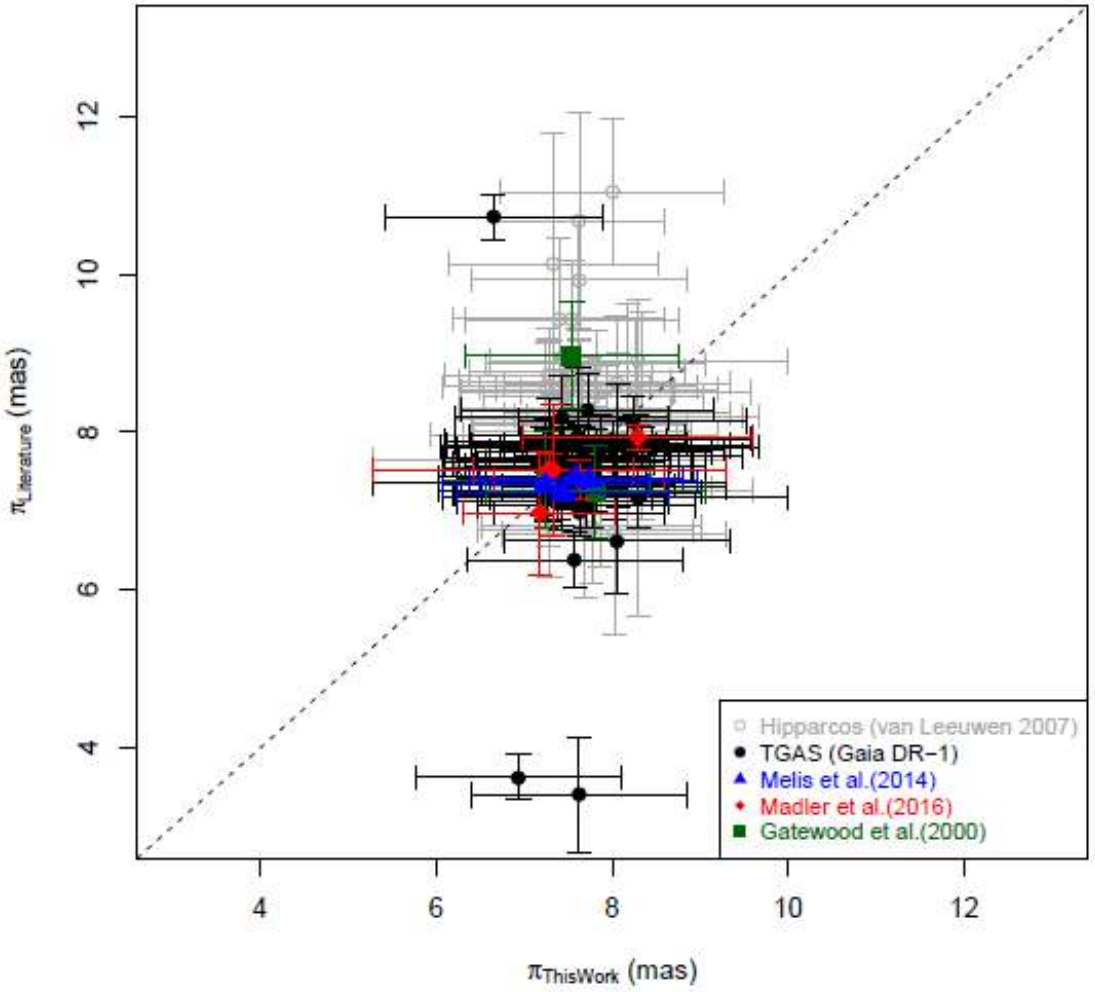

Fig. 16. Comparison between the kinematic parallaxes derived in this work and parallaxes from the literature (van Leeuwen 2007; Melis et al. 2014; Mädler et al. 2016; Gatewood et al. 2000; Gaia Collaboration et al. 2016). The black dashed line indicates the expected distribution for equal results.

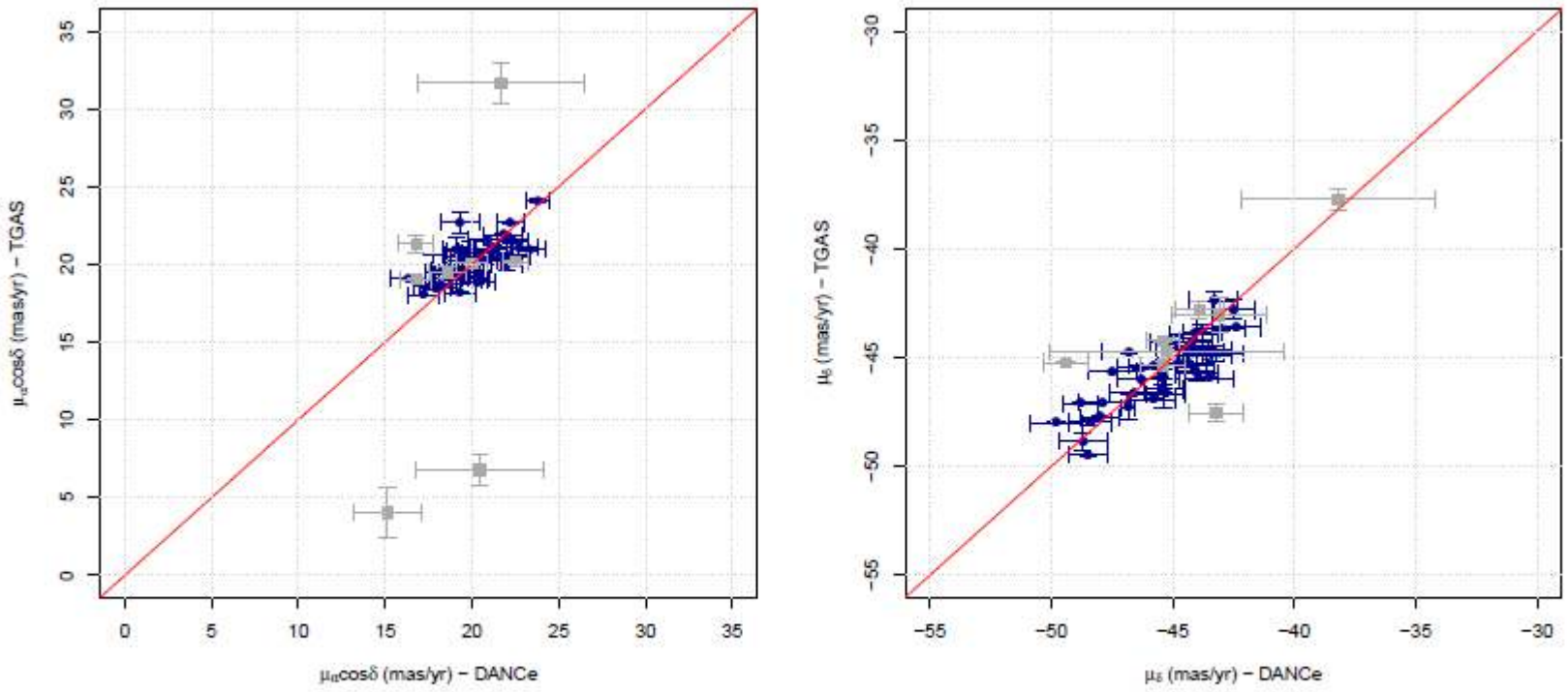

Fig. 17. Comparison between the proper motions measurements in right ascension *(left panel)* and declination *(right panel)* from the DANCe project and the TGAS catalog. The gray squares indicate the discrepant stars listed in Table 8.

120 ± 1.9 pc (HIPPARC
136.2 ± 1.2 pc (VLBI)
133 ± 5 pc (TGAS DR1)
134.4+2.9-2.8 pc (this

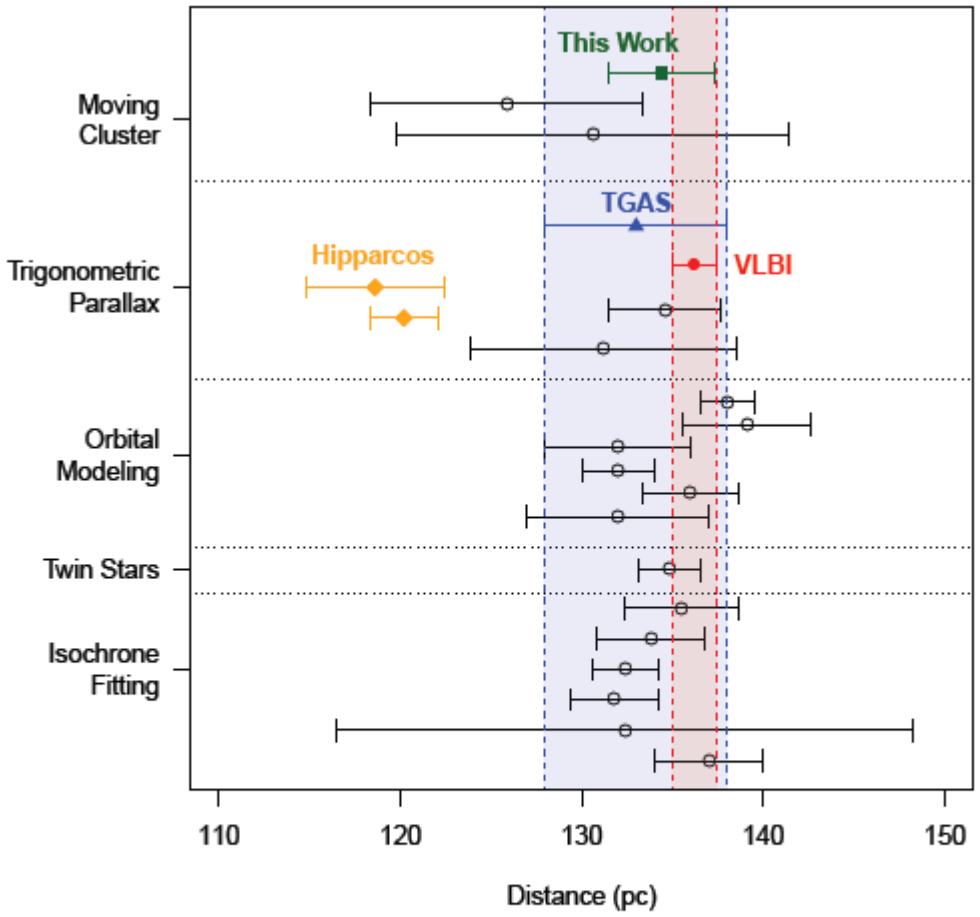

Fig. 18. Summary of distance measurements in the literature for the Pleiades open cluster obtained from different methods. The results presented here come from: (i) *moving cluster* - This Work (see Sect. 5.1), Röser & Schilbach (2013), Narayanan & Gould (1999), (ii) *trigonometric parallax* - van Leeuwen (1999), van Leeuwen (2009), Melis et al. (2014), Soderblom et al. (2005), Gatewood et al. (2000), TGAS (Gaia Collaboration et al. 2016) - using result reported in this work (see Sect. 6.2), (iii) *orbital modeling* - Groenewegen et al. (2007), Southworth et al. (2005), Zwahlen et al. (2004), Munari et al. (2004), Pan et al. (2004), David et al. (2016), (iv) *twin stars*- Mädler et al. (2016), (v) *isochrone fitting* - An et al. (2007), Percival et al. (2005), Stello & Nissen (2001), Pinsonneault et al. (1998), Giannuzzi (1995) and Nicolet (1981),

ATLASGAL – A systematic Survey for Embedded Protoclusters in the Inner Galaxy

Karl Menten

The Atacama Pathfinder Experiment (APEX)

Built and operated (since Sept. 2005) by
- Max-Planck-Institut für Radioastronomie
- Onsala Space Observatory
- European Southern Observatory

on
Llano de Chajnantor (Chile)
Longitude: 67° 45' 33.2" W
Latitude: 23° 00' 20.7" S
Altitude: 5098.0 m

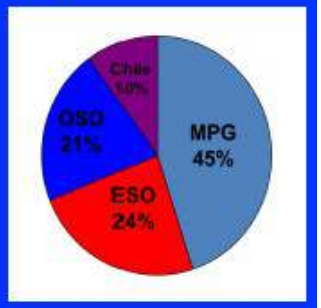

- Dish diameter: 12 m
- Wavelength coverage = 0.2 – 2 mm
- 15 micron rms surface accuracy
- In operation since September 2005
- PI and facility instruments:
  - 230/345 GHz heterodyne RXs
  - 295 element 870 micron Large Apex Bolometer Camera (LABOCA)
  - 37 element Submillimeter Bolometer Camera (SABOCA)

http://www.apex-telescope.org

Distribution of Known Open Stellar Clusters

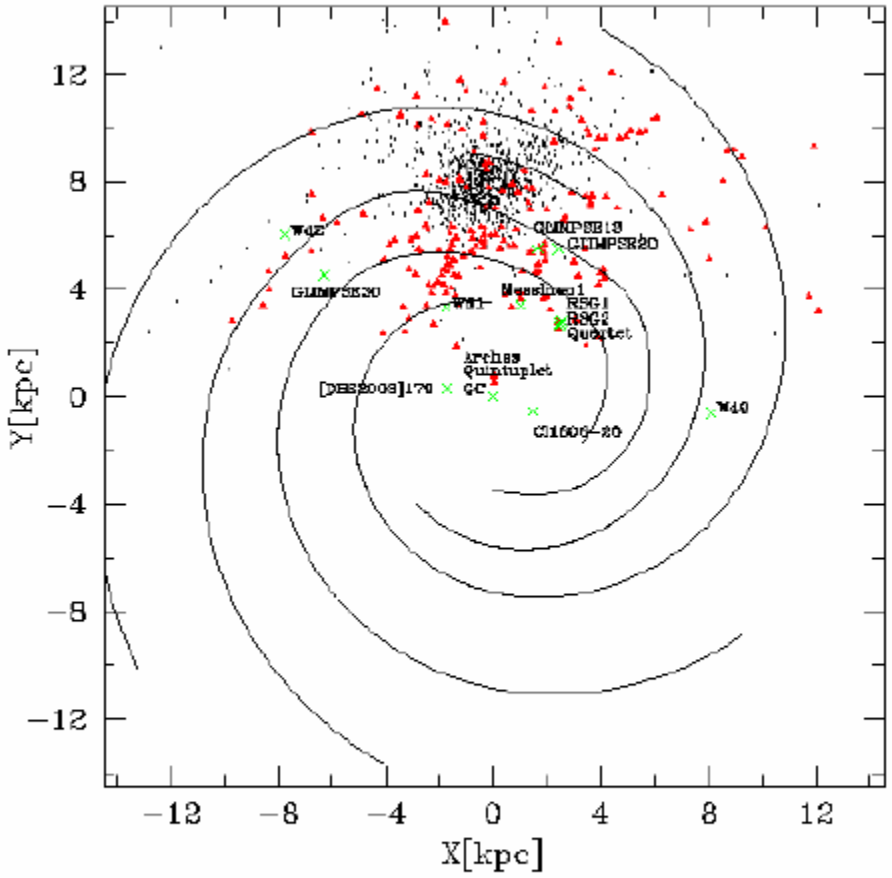

- IR clusters
- Optical clusters
- Massive young clusters($M > 10^4 M_\odot$)

Compilation:
M. Messineo

Infrared candidate clusters can probe the inner Galaxy

ATLASGAL – Short Description:

- Unbiased survey of the inner Galactic Plane at 870 μm
- **Main goals :**
  - study massive star formation throughout the Galaxy
  - pre-stellar initial mass function down to a few $M_\odot$
  - study large scale structure of the cold ISM
  - associate w. other Galactic surveys (Spitzer, MSX, Hi-GAL)

IRAS 12+60+100 μm, $|l| \leq 90°$, $|b| \leq 10°$

- Mapping $|l| \leq 60°$, $|b| \leq 1.5°$, sensitivity 1-σ = 50 mJy/beam

➔360 deg^2, 5σ detection:
0.5 $M_\odot$at 500 pc, 20 $M_\odot$at 3 kpc, 100 $M_\odot$at 8 kpc

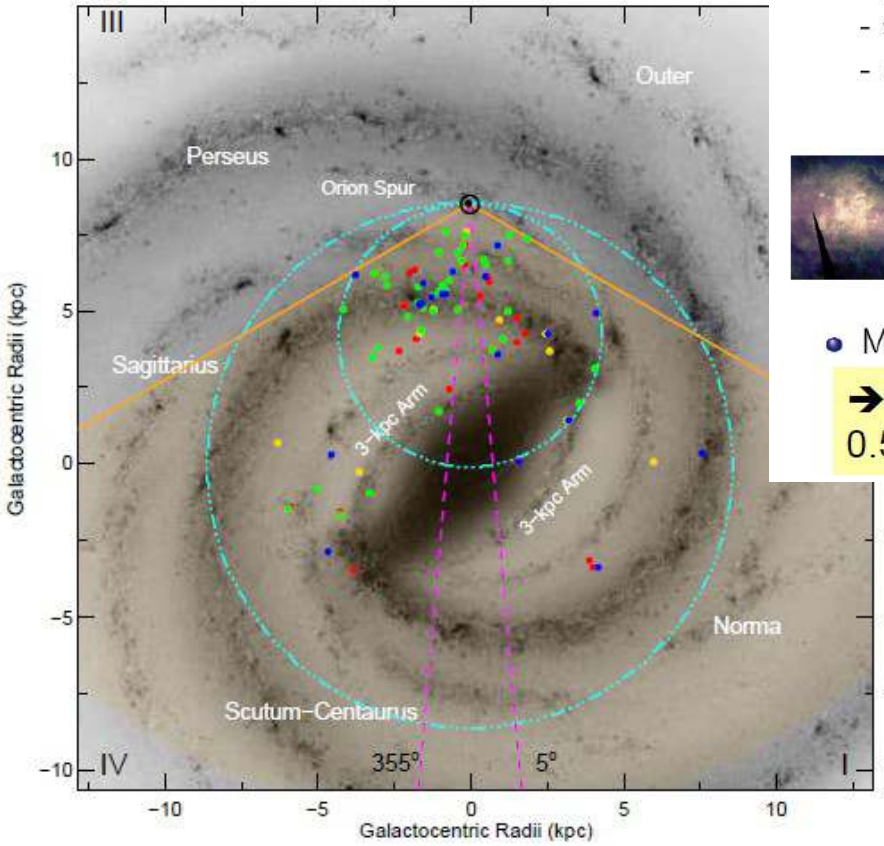

Fig. 3. Galactic distribution of the ATLASGAL Top100 sample. The positions of the H II regions, mid-infrared bright, mid-infrared weak and 70 μm weak sources are indicated by the blue, green and red and yellow filled circles, respectively. The orange shaded area indicates the region of the Galactic plane covered by the ATLASGAL survey to a distance of 20 kpc, within which the survey is complete for compact clumps with masses >1000 $M_\odot$. The background image is a schematic of the Galactic disc as viewed from the Northern Galactic Pole (cour

arXiv:1610.09055

Spectroscopic evidence of Multiple Stellar Population in Globular Clusters

Eugenio Carreta

arXiv:1611.04728

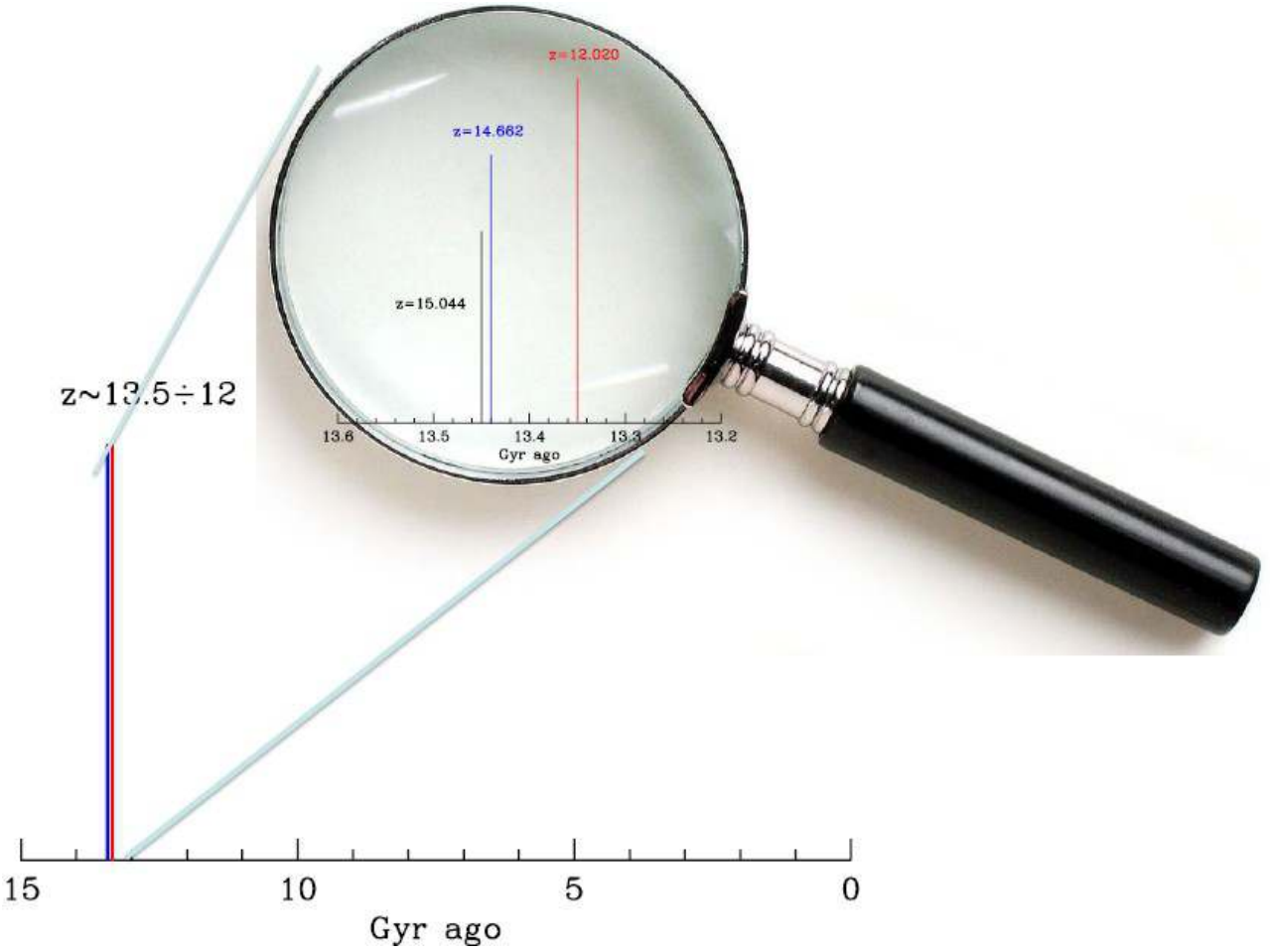

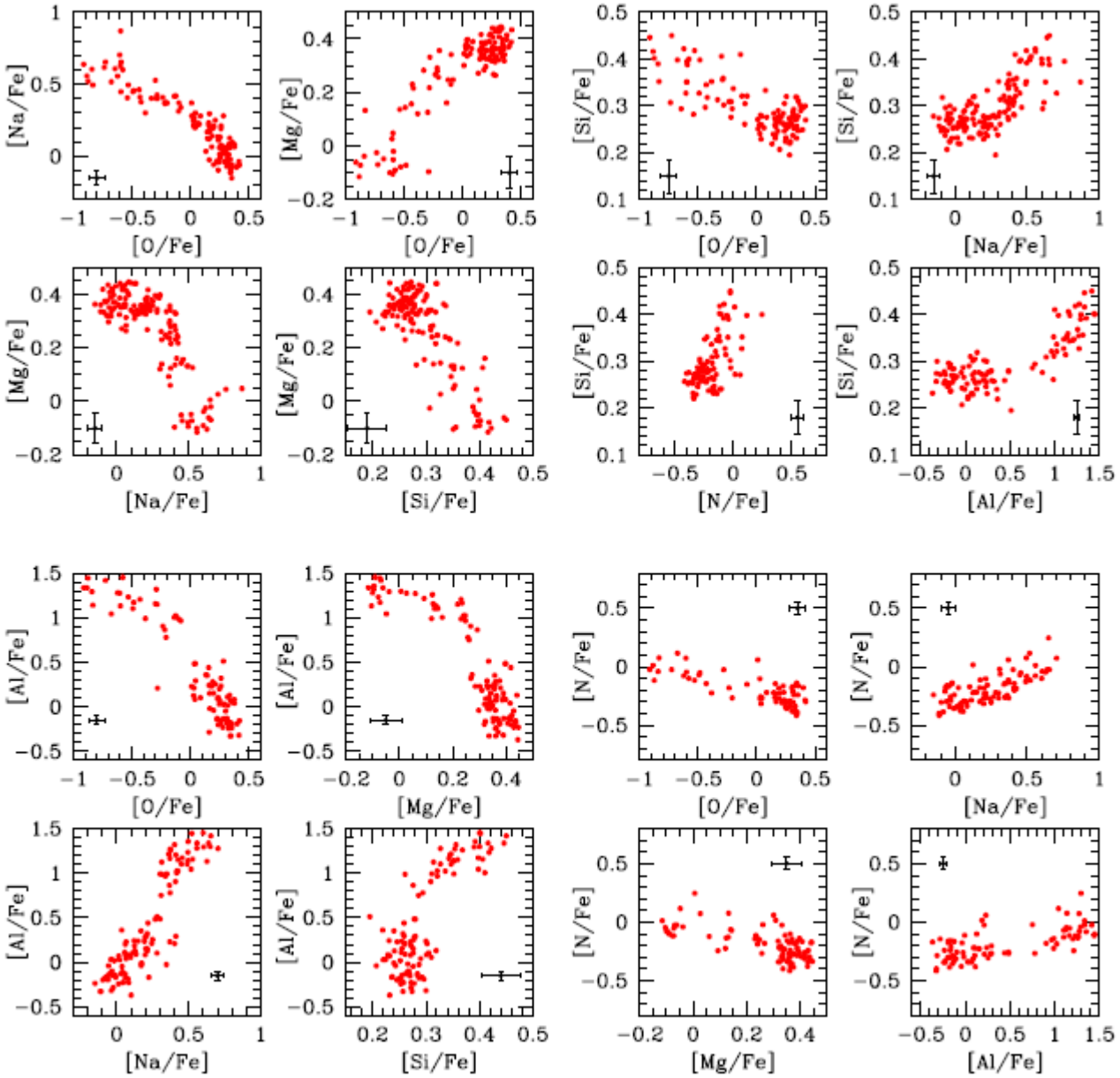

Figure 1: Trends of abundance ratios for light elements in RGB stars of NGC 2808. O, Na, Si, Mg are from Carretta (2015), Al and N abundances from Carretta et al. (in prep.).

Do we know a common process able to explain all the observed patterns? Yes: the origin of these signature was identified in proton capture reactions in hydrogen burning at high temperature, where several synthesis chains are simultaneously active (Denisenkov & Denisenkova 1989, Langer et al. 1993). However, the required temperatures are high ($> 40 \times 10^6$ K for the ON and NeNa cycles, and even higher for the MgAl cycle, $T > 70 \times 10^6$ K), not reached in the interior of the presently observed GC low mass stars. The implication is that this nuclear burning occurred in stars more massive than those evolving today, and this is the reason why since Gratton et al. (2001) discovered the Na-O and Mg-Al anticorrelations among unevolved GC stars (Figure 3), these (anti)correlations *are simply an alias for multiple stellar populations.*

In summary, with respect to abundances from Supernovae:

C,O,Mg (not always) decrease in second generation stars

and simultaneously

N,Na,Al (not always),K, Sc (not always) increase in second generation stars

(anti)correlations among light elements (C to Si,K,Sc)

Where?

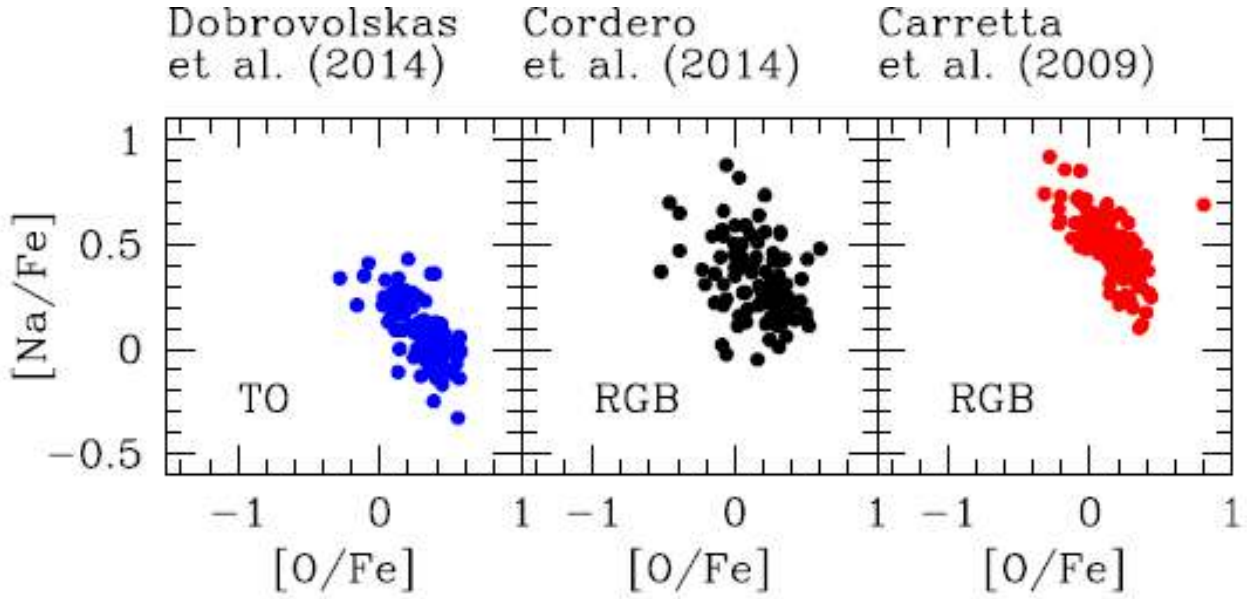

Figure 6: Na-O anticorrelation in 47 Tuc for main sequence/turnoff stars from Dobrovolskas et al. (left panel) and for RGB stars from Cordero et al. (2014) and Carretta et al. (2009), central and right panels, respectively.

Where in the Galaxy?

Halo/Bulge/Thick disk

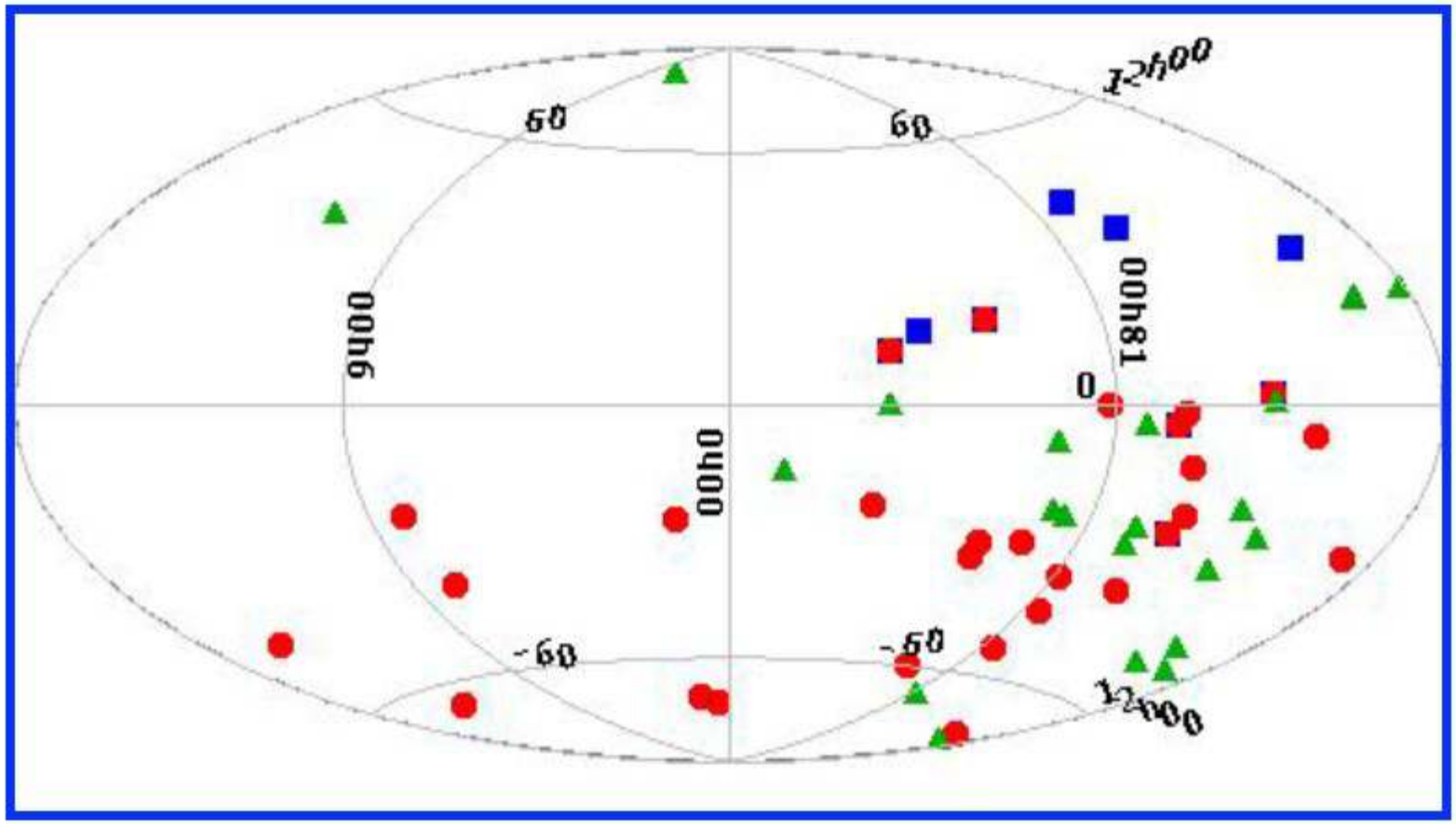

Lick-Texas

FLAMES survey

FLAMES & Lick-Texas

other groups

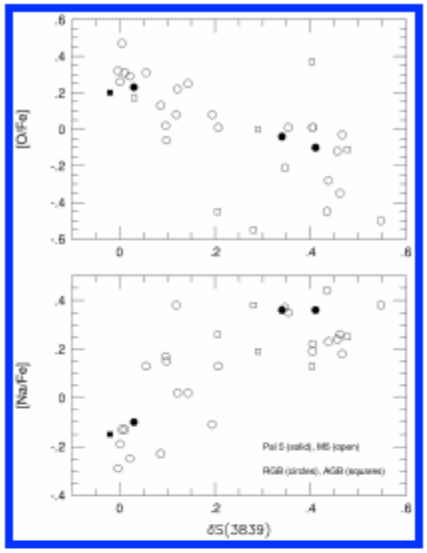

Pal 5 (Smith et al. 2002)

Mv= -5.17

Mass

~10000 Mo

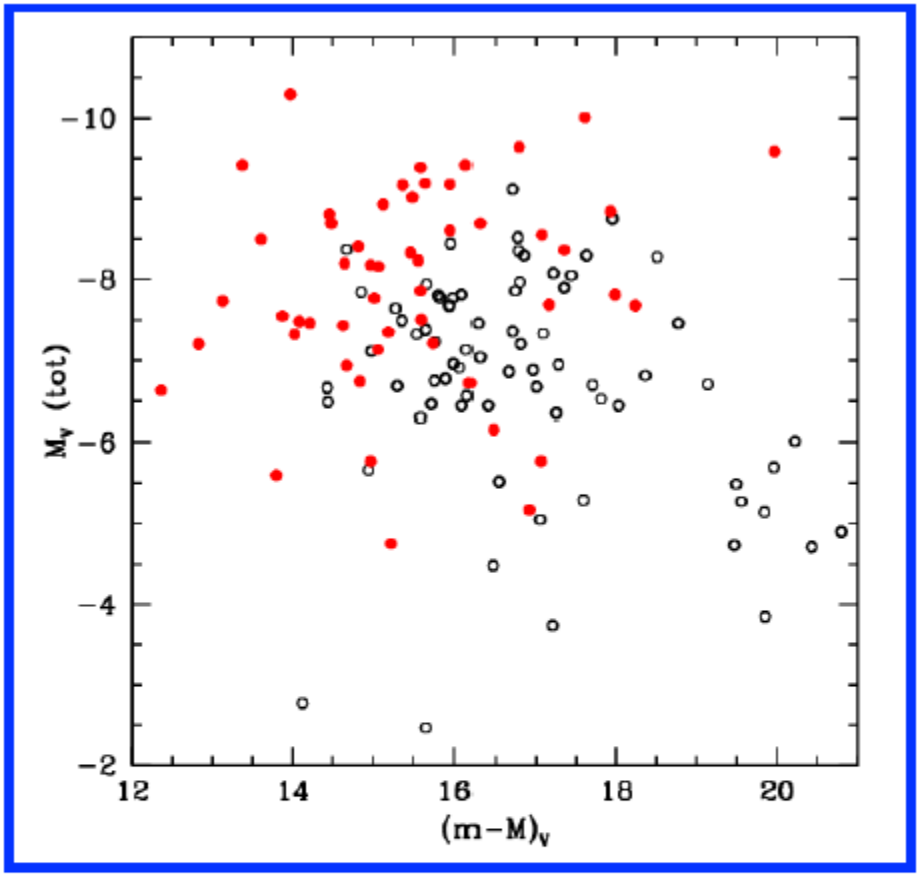

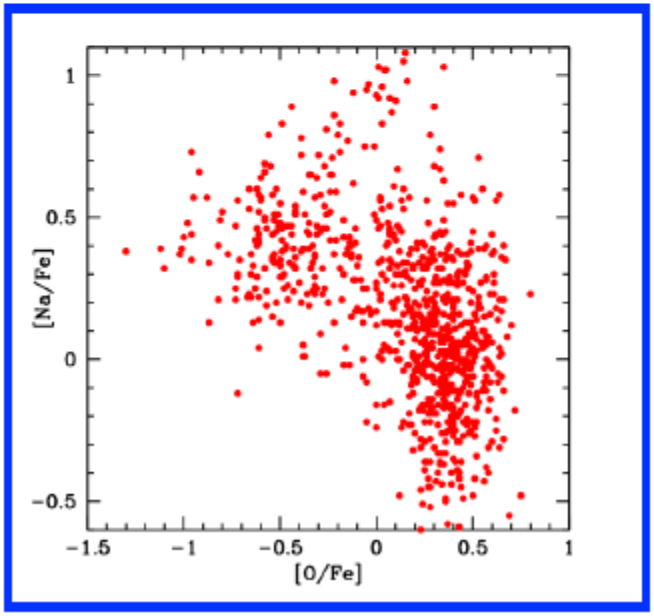

ω Cen (Johnson & Pilachowski 2010, Marino et al. 2011)

Mv= -10.29

Mass ~ 2.3 x 10^6 Mo

Extragalactic old globular clusters

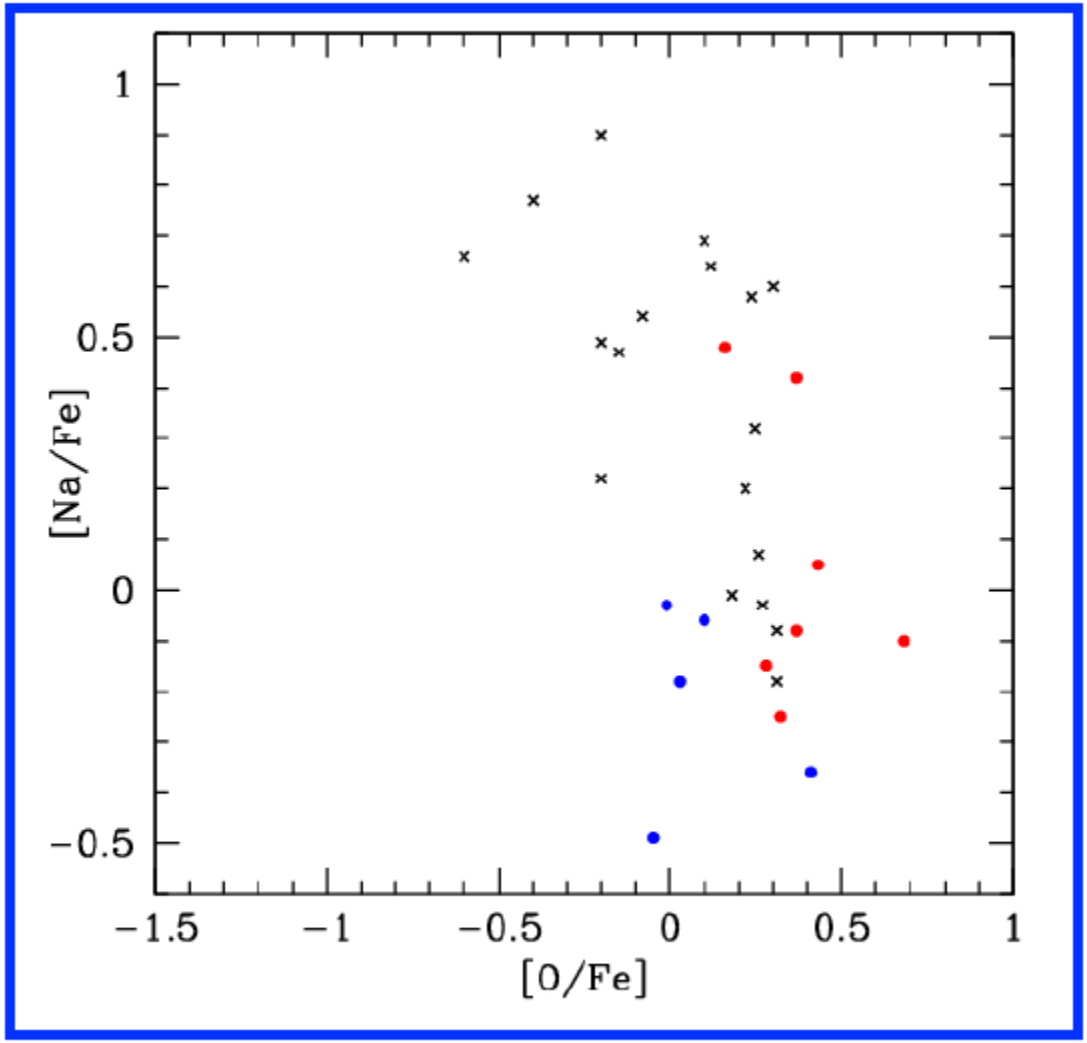

Johnson et al. (2006):
4 old LMC GCs

Letarte et al. (2006):
3 GCs in Fornax dSph

Mucciarelli et al. (2009):
3 old LMC GCs

No evidence of self-enrichment in intermediate-age LMC clusters (Mucciarelli et al. 2008)

Iron complex GCs: clusters with small/moderate (and correlated) Fe & s-process element spreads

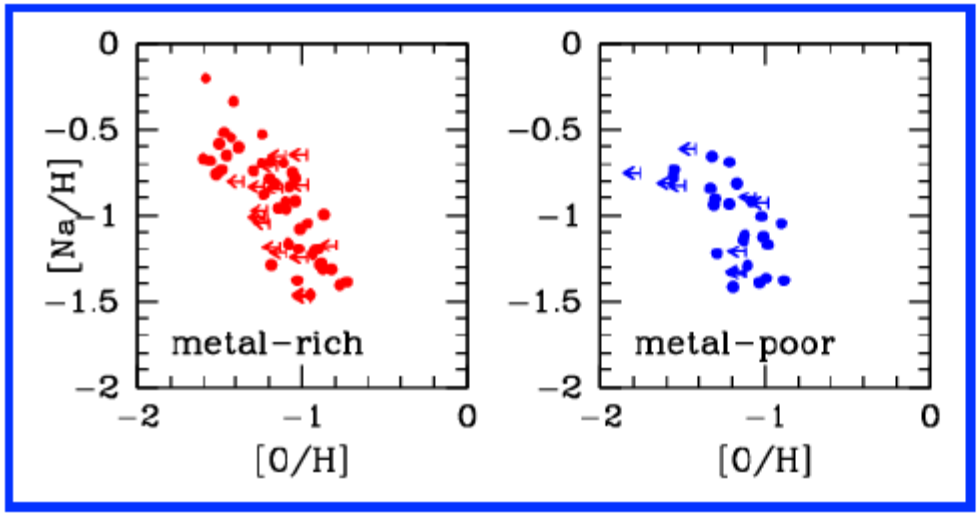

NGC 1851
Carretta et al. (2011)

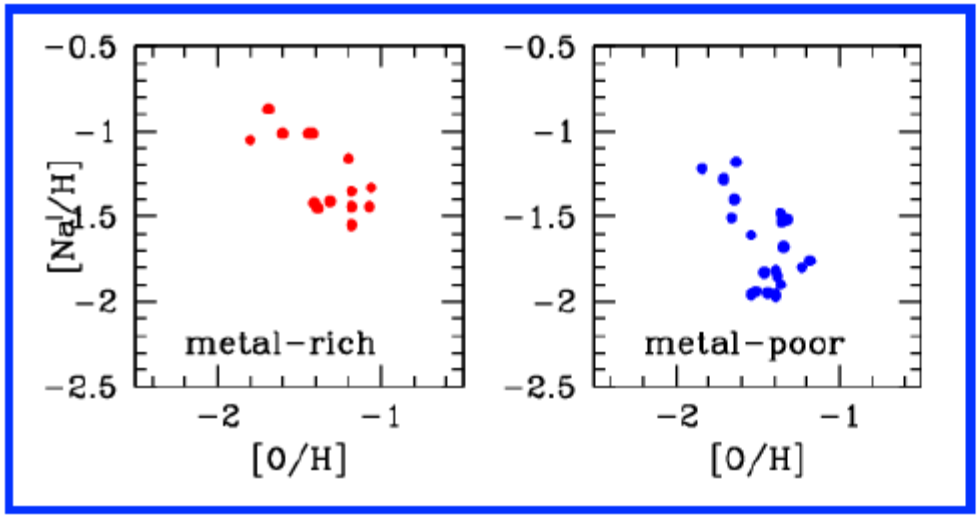

M 22
Marino et al. (2011)

M 2 Yong et al. (2014); NGC 5286 Marino et al. (2015), NGC 5824 (Roederer et al. (2015), M 19 Johnson et al. (2015)

Large stellar systems with a metallicity dispersion: galaxies or globular clusters?

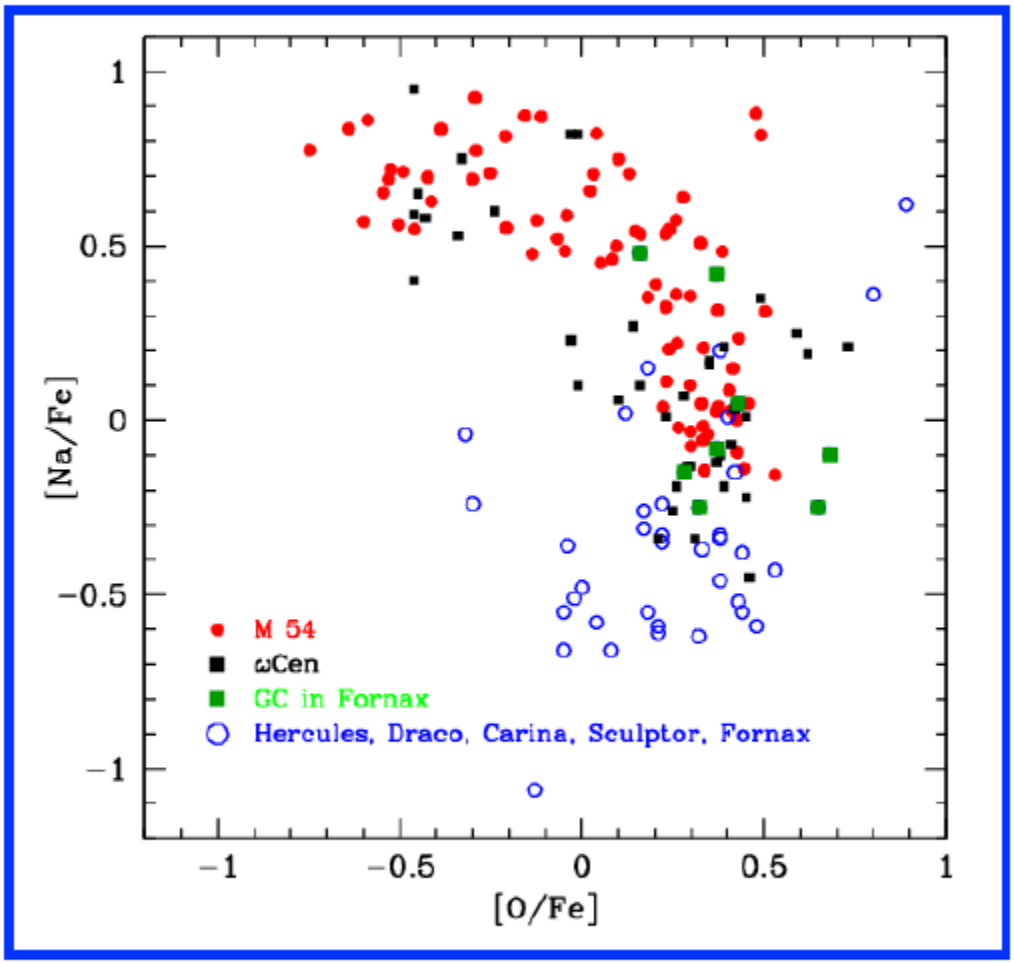

	Dist.(kpc)	Mv	Na-O
Carina	101	-9.3	no
Sculptor	86	-11.2	no
UMinor	70	-9.0	no
Draco	76	-8.6	no
Fornax	138	-13.2	no
ω Cen	5	-10.3	yes
M 54	26	-10.0	yes

Anticorrelation limited to GCs

Carretta et al. (2011), Norris & Da Costa (1995), Letarte et al. (2006). Shetrone et al. (2001,2003), Cohen & Huang (2009), Koch et al. (2008), Geisler et al. (2004)

The Na-O anticorrelation found in:

NGC 288

NGC 362

NGC 1851

NGC 2808

NGC 3201

NGC 4833

NGC 6397

M3, M4, M5, M10,
M13, M15, M22, M30,
M54, M55, M 68, M92

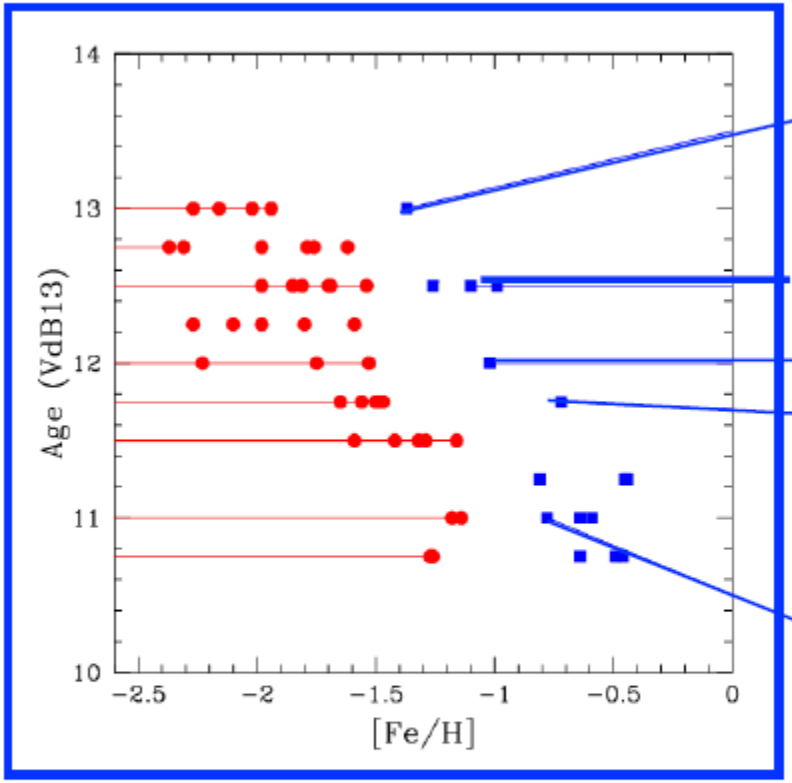

ACCRETED

VandenBerg et al. (2013), Leaman et al. (2013)
(see also Marin-Franch et al. 2009)

IN SITU

INTRINSIC SIGNATURE OF A BONA FIDE GC

Carretta et al. (2010)

Total mass = driving parameter

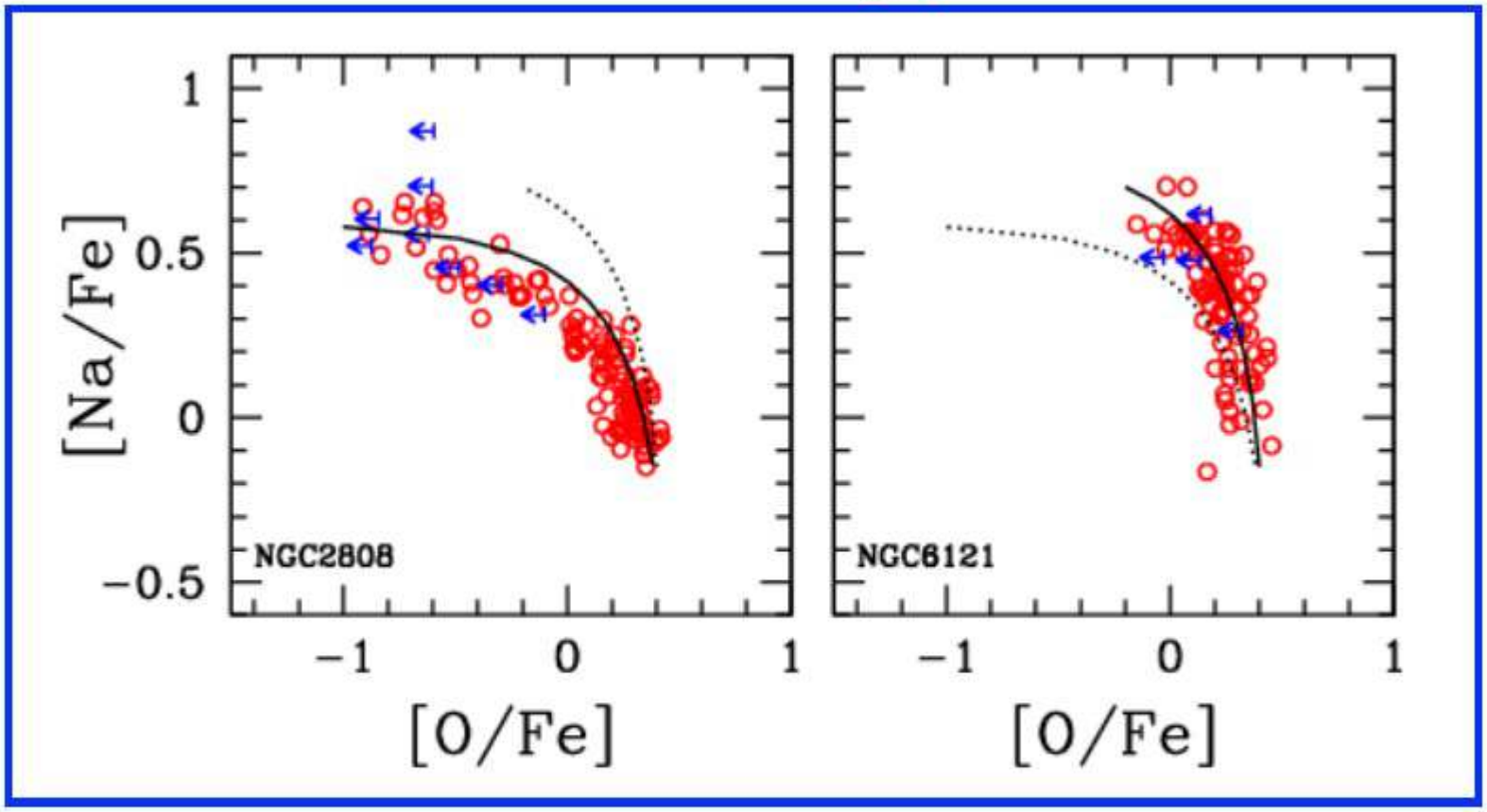

[Fe/H] = -1.15 dex

[Fe/H] = -1.17 dex

Mv (tot) = -9.39

Mv (tot) = -7.19

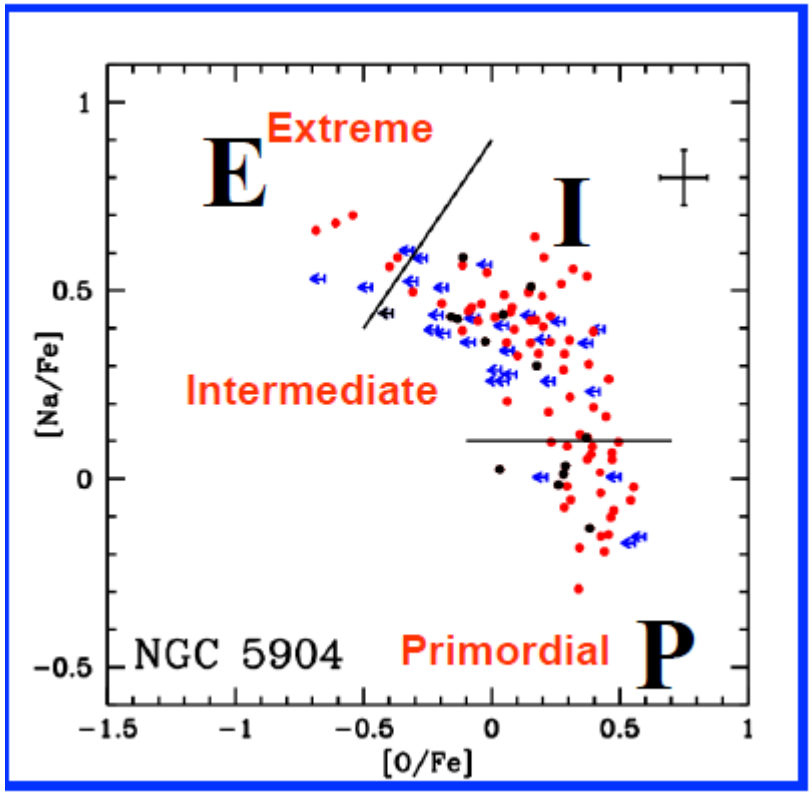
E
Extreme
I
Intermediate
P
Primordial
NGC 5904
[Na/Fe]
[O/Fe]
1
0.5
0
−0.5
−1.5
−1
−0.5
0
0.5
1

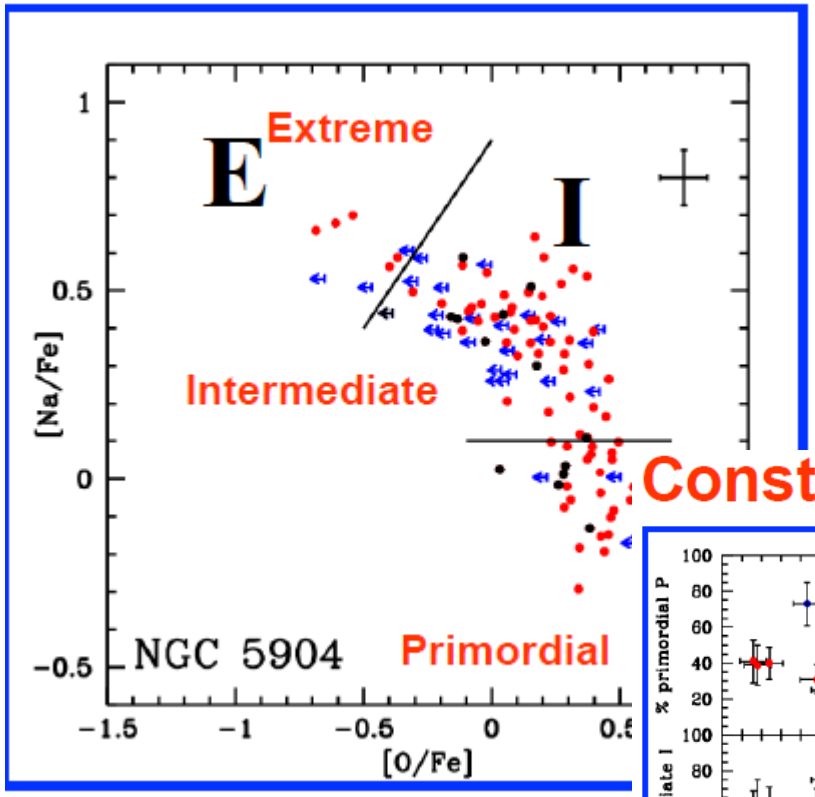

Constraints on GC mass

P ≅ 33% I ≅ 50-70%

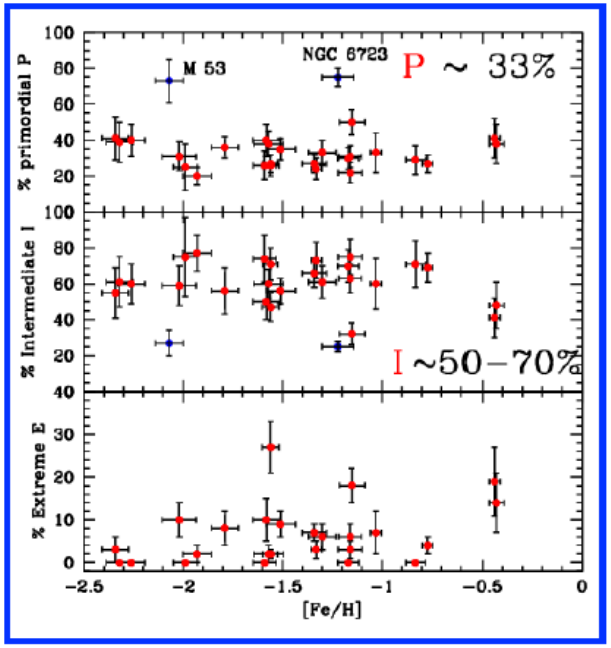

The most massive P stars contribute to form second generation stars (I,E), currently 2/3 of GC stars

Mass budget problem

- precursor of GCs were 10-20 times more massive than present end products (Bekki et al. 2007 and many others) and
- proto-GC lost ~90% of their stars → possibly main contribution to halo

Furthermore, simulations of mass loss from gas expulsion predict a strong anticorrelation between the fraction of SG stars and the cluster mass, that is not observed (Khalaj and Baumgardt 2015), and no variation of the fraction of SG as a function of cluster mass or galactocentric distance or metallicity is observed (Kruijssen 2015, Bastian and Lardo 2015), at odds with what expected by mechanisms of mass loss.

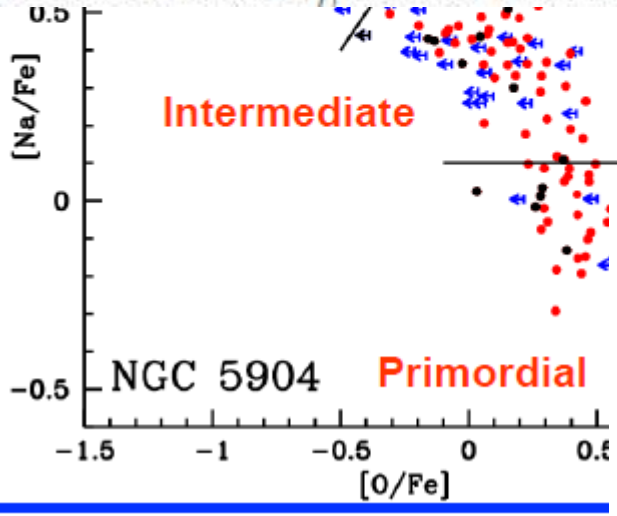

Constraints on GC mass

P ≅ 33% **I ≅ 50-70%**

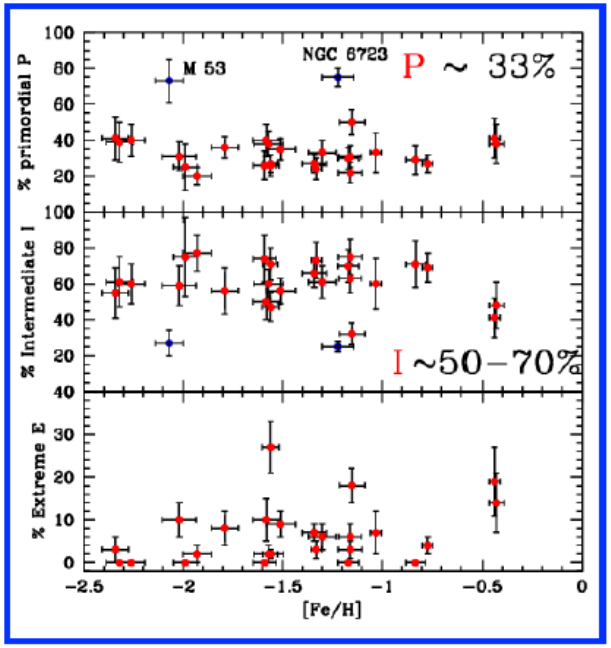

The most massive P stars contribute to form second generation stars (I,E), currently 2/3 of GC stars

Mass budget problem

- **precursor of GCs were 10-20 times more massive than present end products (Bekki et al. 2007 and many others) and**
- **proto-GC lost ~90% of their stars → possibly main contribution to halo**

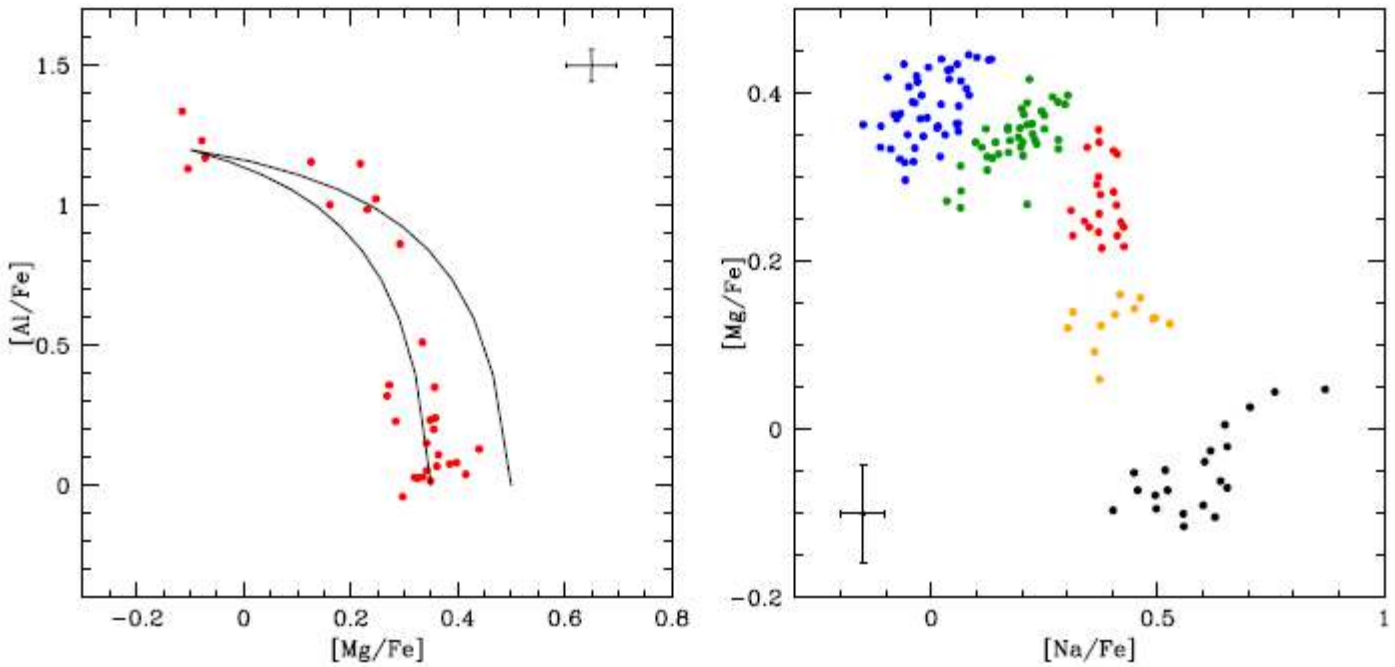

Figure 19: [Al/Fe] ratios as a function of [Mg/Fe] ratios in NGC 2808 (Carretta 2014, left panel) with superimposed two dilution models. No single dilution model is able to fit all the three components. Right panel: five groups with distinct chemical composition on the RGB of NGC 2808 from Carretta (2015).

Finally, it appears to be difficult to account for all the combined spectroscopic and photometric evidence within a single scenario (e.g. Bastian et al. 2015). In particular, the discrete components seen by spectroscopic observations in some clusters (NGC 6752, Carretta et al. 2012a; NGC 2808, Carretta 2014 2015, see Figure 19) suggest that a dilution model with only one class of polluters could not be enough for all components.

So, in conclusion taking into account the large variety of chemical signatures in GCs (spread in light elements, always; also in heavier elements and metallicity, in some cases) the most honest summary I can give you from the spectroscopic evidence is this: a genuine, *bona fide* old globular cluster is a system where a chain of events (not yet well understood) concurred to form at least two stellar generations with small age differences and huge variations in the content of products of hot H-burning nucleosynthesis.

Multiple Stellar Populations in Young and Old Globular Clusters

Antonino Milone

The *Hubble Space Telescope* UV Legacy Survey of Galactic Globular Clusters. IX. The Atlas of Multiple Stellar Populations.

A.P. Milone + arXiv:1610.00451

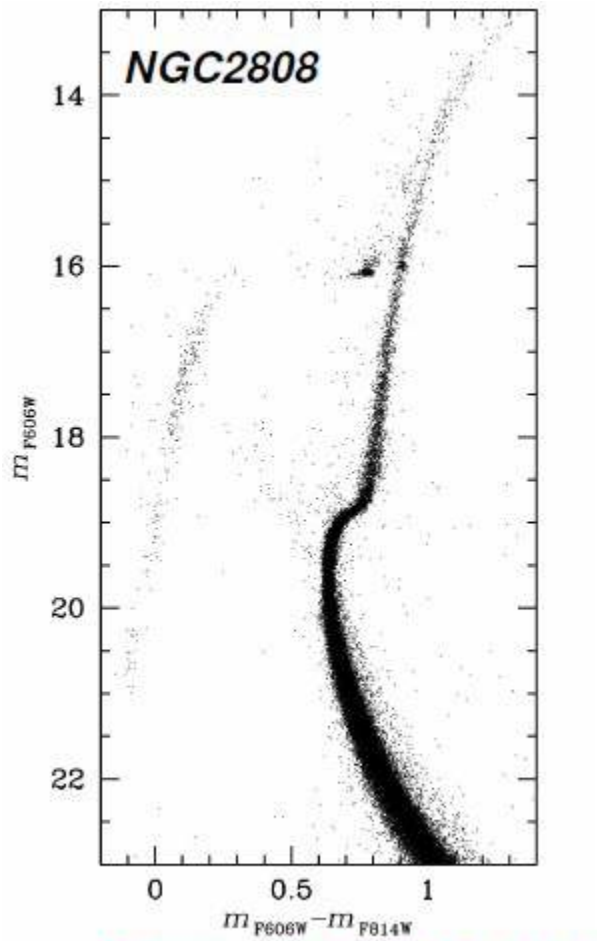

Anderson et al. 2008, AJ, 135, 2055

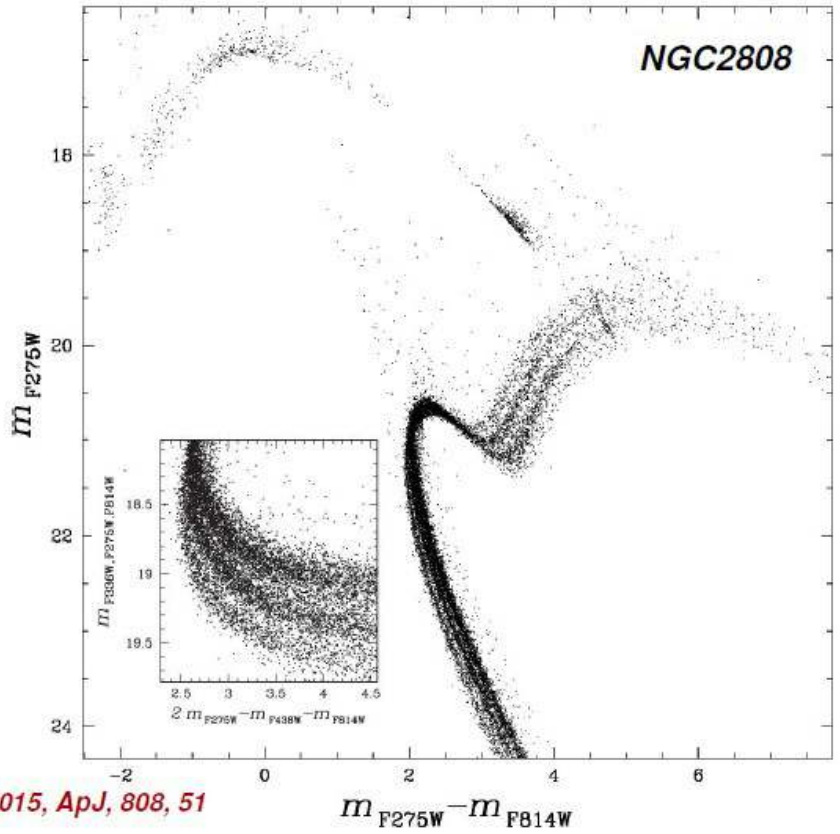

Milone et al. 2015, ApJ, 808, 51

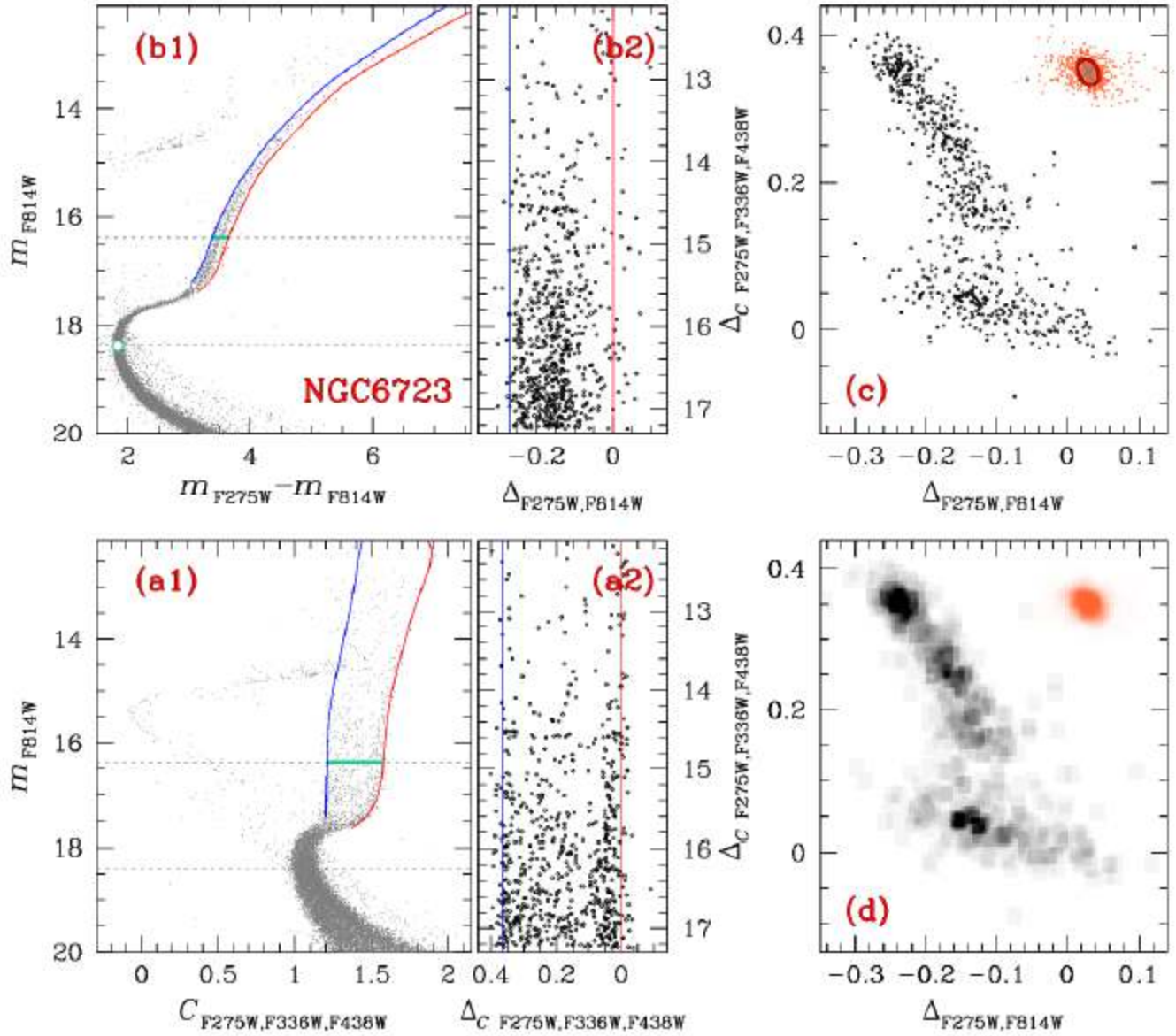

Figure 1. This figure illustrates the procedure to derive the $\Delta_{F275W,F336W,F438W}$ vs. $\Delta_{F275W,F814W}$ pseudo two-color diagram (or 'chromosome map') for the prototypical cluster NGC 6723. Panels (a1) and (b1) show the the m_{F814W} vs. $C_{F275W,F336W,F438W}$ pseudo-CMD and the m_{F814W} vs. $m_{F275W} - m_{F814W}$ CMD of NGC 6723. The aqua circle in panel (b1) marks the MS turn-off, whereas the two horizontal dotted lines in panels (a1) and (b1) are placed at the magnitude level of the MS turn-off and 2.0 F814W mag above it. The blue and red lines mark the boundaries of the RGB, while the aqua segments in the panels (a1) and (b1) indicate the $m_{F275W} - m_{F814W}$ color and the $C_{F275W,F336W,F438W}$ pseudo-color separation between the two lines at 2.0 F814W mag above the MS turn off. The 'verticalized' m_{F814W} vs. $\Delta_{C\ F275W,F336W,F438W}$ and m_{F814W} vs. $\Delta_{F275W,F814W}$ diagrams for RGB stars are plotted in panels (a2) and (b2), respectively,

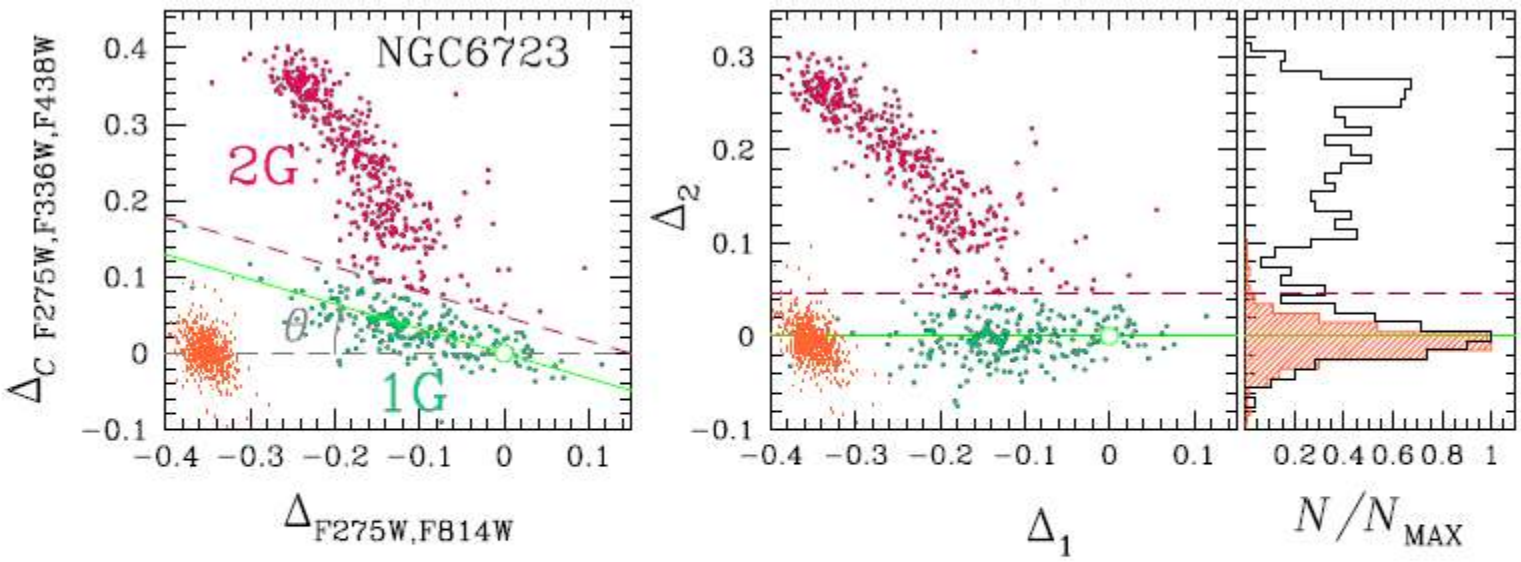

Figure 2. The figure illustrates the method used to identify the two samples of bona-fide first generation (1G) and second generation (2G) stars in NGC 6723. The left panel reproduces the $\Delta_{F275W,F336W,F438W}$ vs. $\Delta_{F275W,F814W}$ diagram from Figure 1. The green line through the origin of the frame is a fit to the sequence of candidate 1G stars and defines an angle $\theta = 18°$ with respect to the horizontal line. The middle panel shows the Δ_2 vs. Δ_1 plot where these new coordinates have been obtained by rotating counterclockwise by an angle θ the plot in the left panel. The histogram in the right panel shows the distributions of the Δ_2 values. The orange points in the left and middle panels show the distribution of the observational errors and their Δ_2 distribution is represented by the shaded orange histogram in the right panel. The dashed magenta lines separate the selected 1G and 2G stars, which are colored aqua and magenta, respectively, in the left and middle panels. See the text for details.

Звезды и 1G, и 2G химически неоднородны – см. на оранжевый эллипс.

Building the Atlas

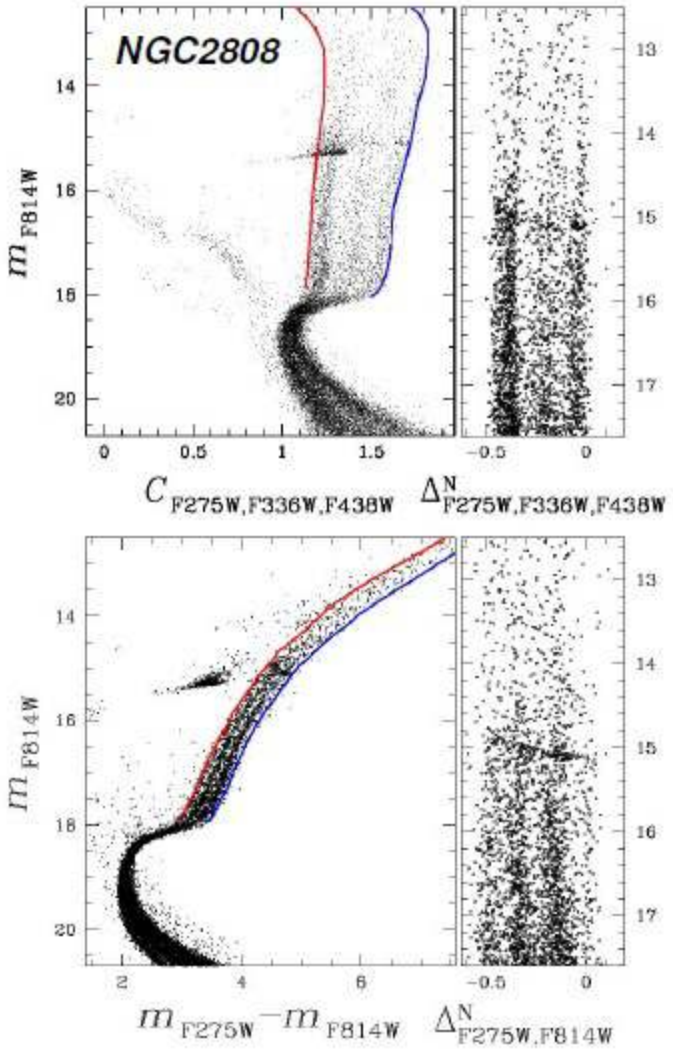

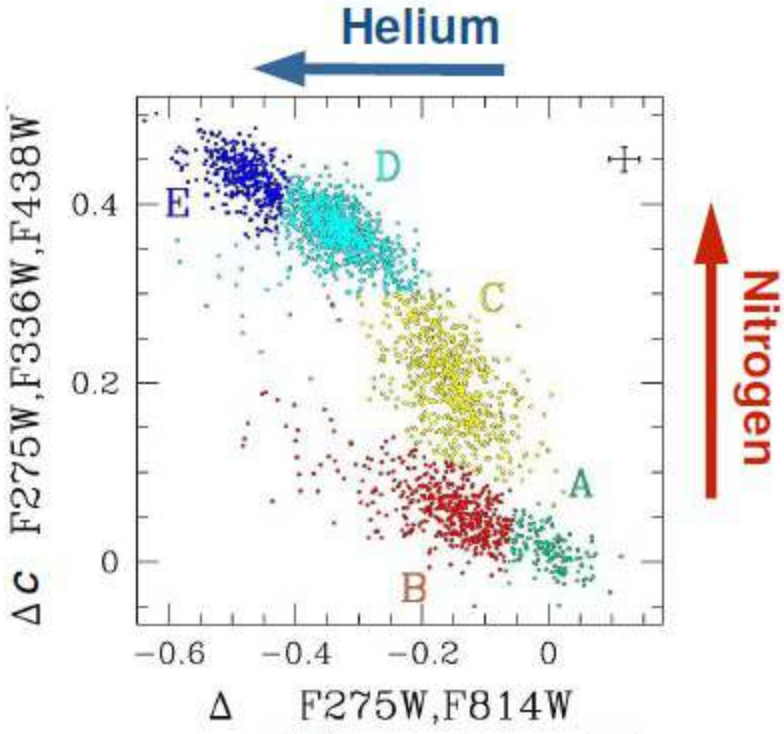

Milone et al. 2015, ApJ, 808, 51

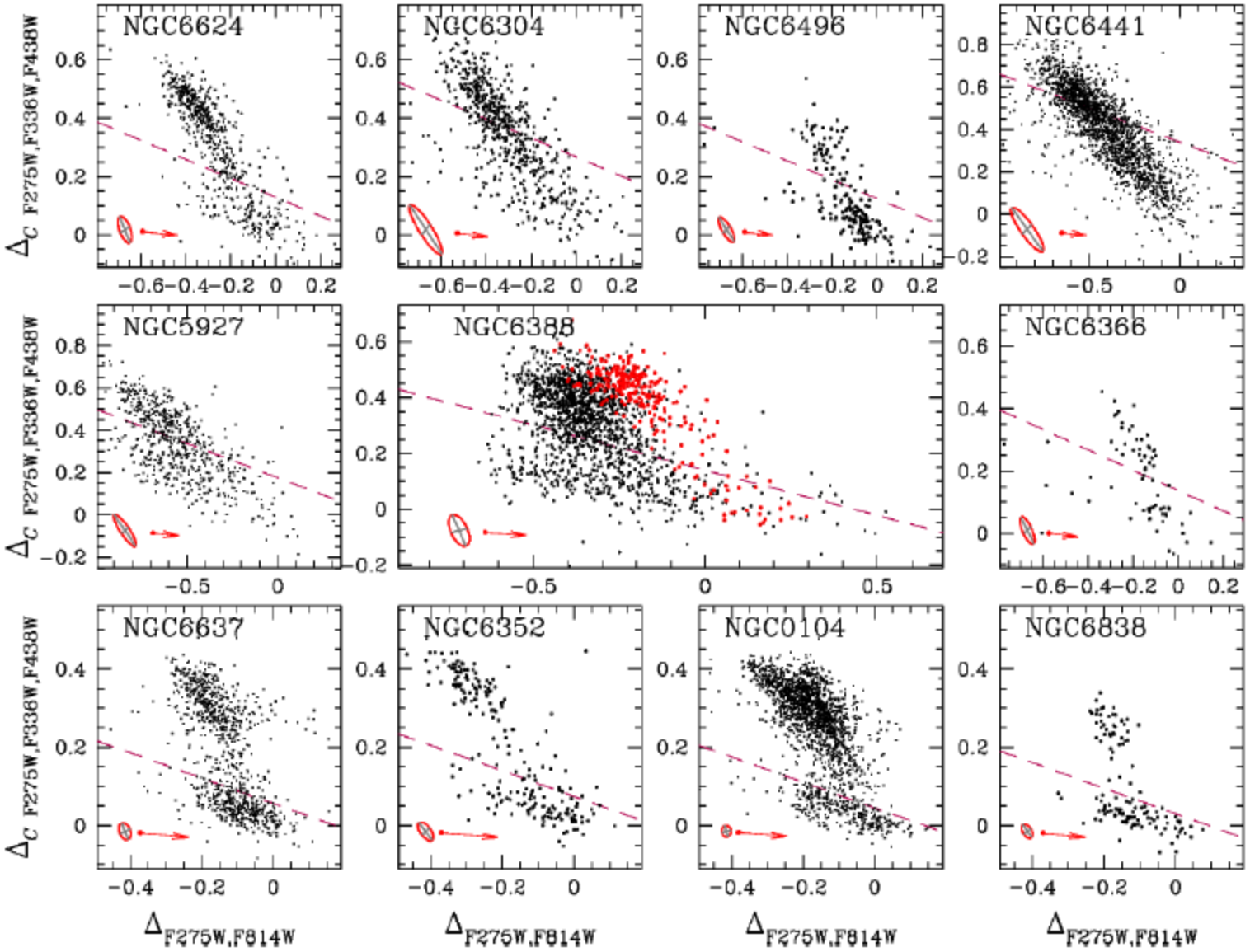

Figure 3. $\Delta_{C\ F275W,F336W,F438W}$ vs. $\Delta_{F275W,F814W}$ diagrams, or chromosome maps, for RGB stars in 11 GCs. Namely NGC 6624, NGC 6304, NGC 6496, NGC 6441, NGC 5927, NGC 6388, NGC 6366, NGC 6637, NGC 6352, NGC 104 (47 Tucanae), and NGC 6838 (M 71). Clusters are approximately sorted according to their metallicity, from the most metal rich, to the most metal poor. The ellipses are indicative of the observational errors and include 68.27% of the simulated stars. The magenta dashed line is used to separate bona-fide 1G from 2G stars and has been determined as in Section 4.2. Red points indicate red-RGB stars and will be selected and discussed in Section 5, while the arrows indicate the reddening vector and correspond to a reddening variation of $\Delta E(B-V)$=0.05. Note, however, that all these plots are constructed using photometric data corrected for differential reddening.

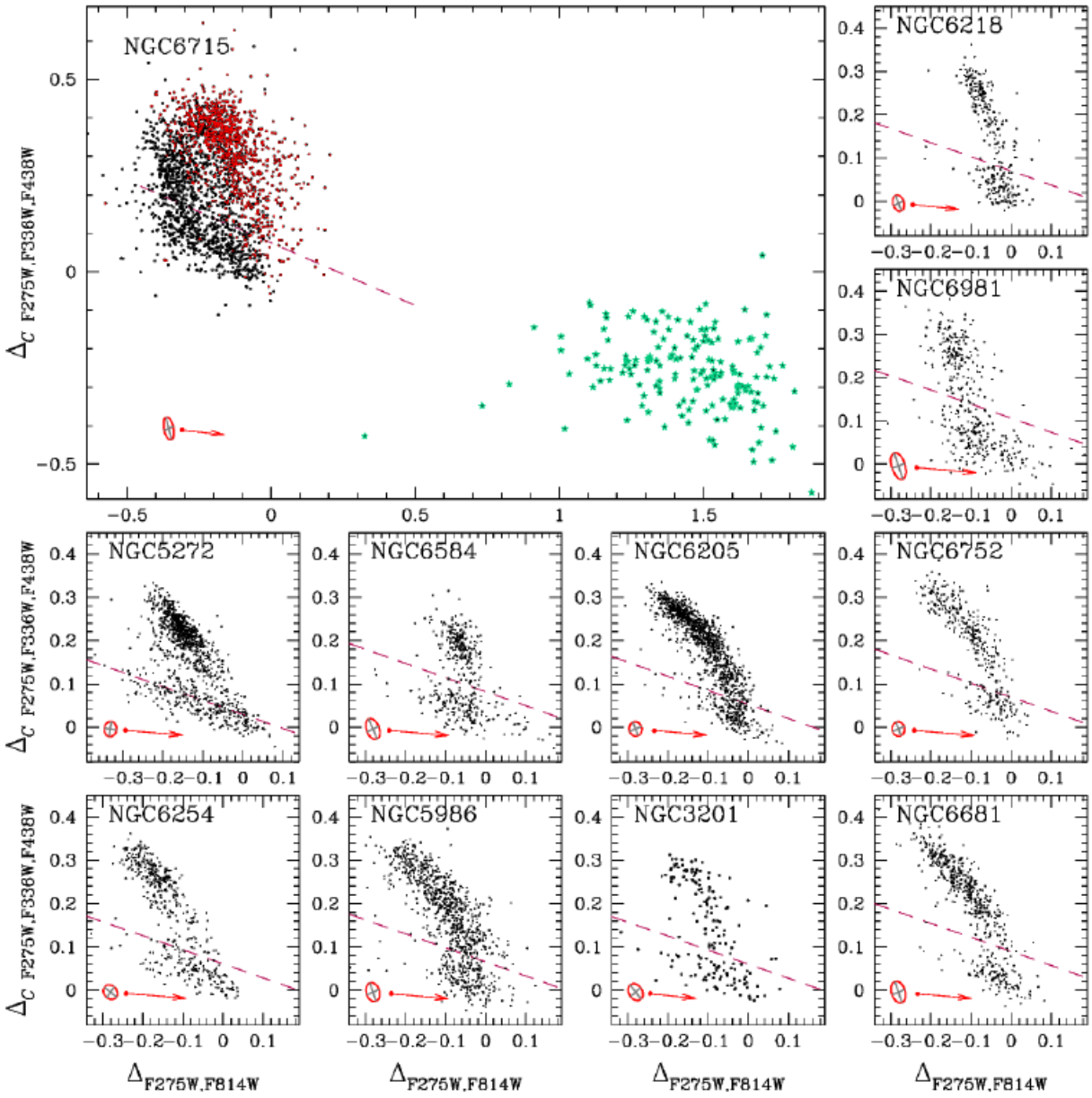

Figure 5. As in Figure 3, but for the stellar system formed by NGC 6715 (M 54), and for NGC 6218 (M 12), NGC 6981 (M 72), NGC 5272 (M 3), NGC 6584, NGC 6205 (M 13), NGC 6752, NGC 6254 (M 10), NGC 5986, NGC 3201, and NGC 6681 (M 70). The aqua starred symbols in the map of M 54 indicate stars of the metal rich population in the core of the Sagittarius dwarf galaxy, to which M54 belongs.

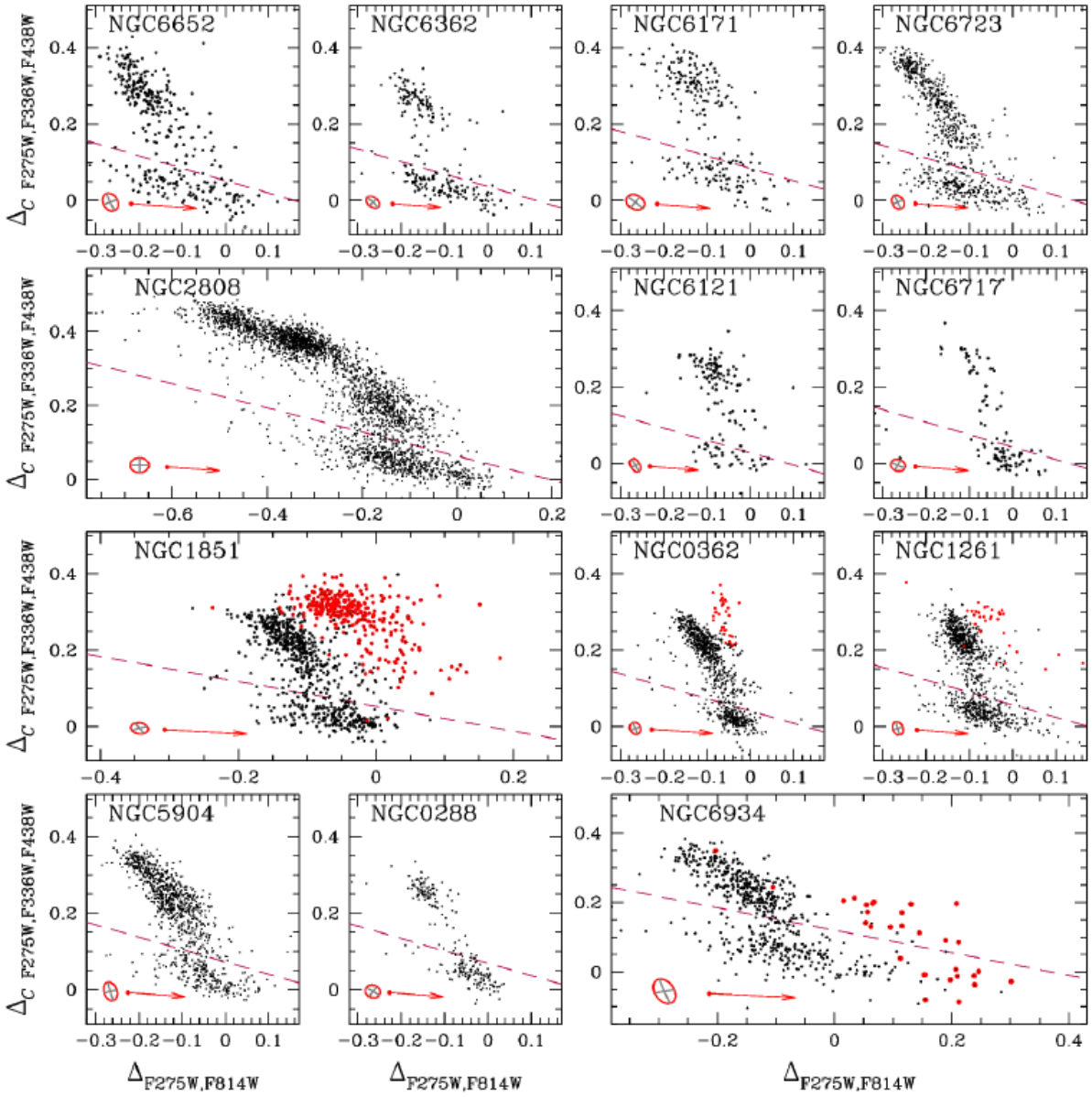

Figure 4. As in Figure 3, but for NGC 6652, NGC 6362, NGC 6171 (M 107), NGC 6723, NGC 2808, NGC 6121 (M 4), NGC 6717, NGC 1851, NGC 362, NGC 1261, NGC 5904 (M 5), NGC 288, and NGC 6934.

The Atlas of multiple populations in GCs

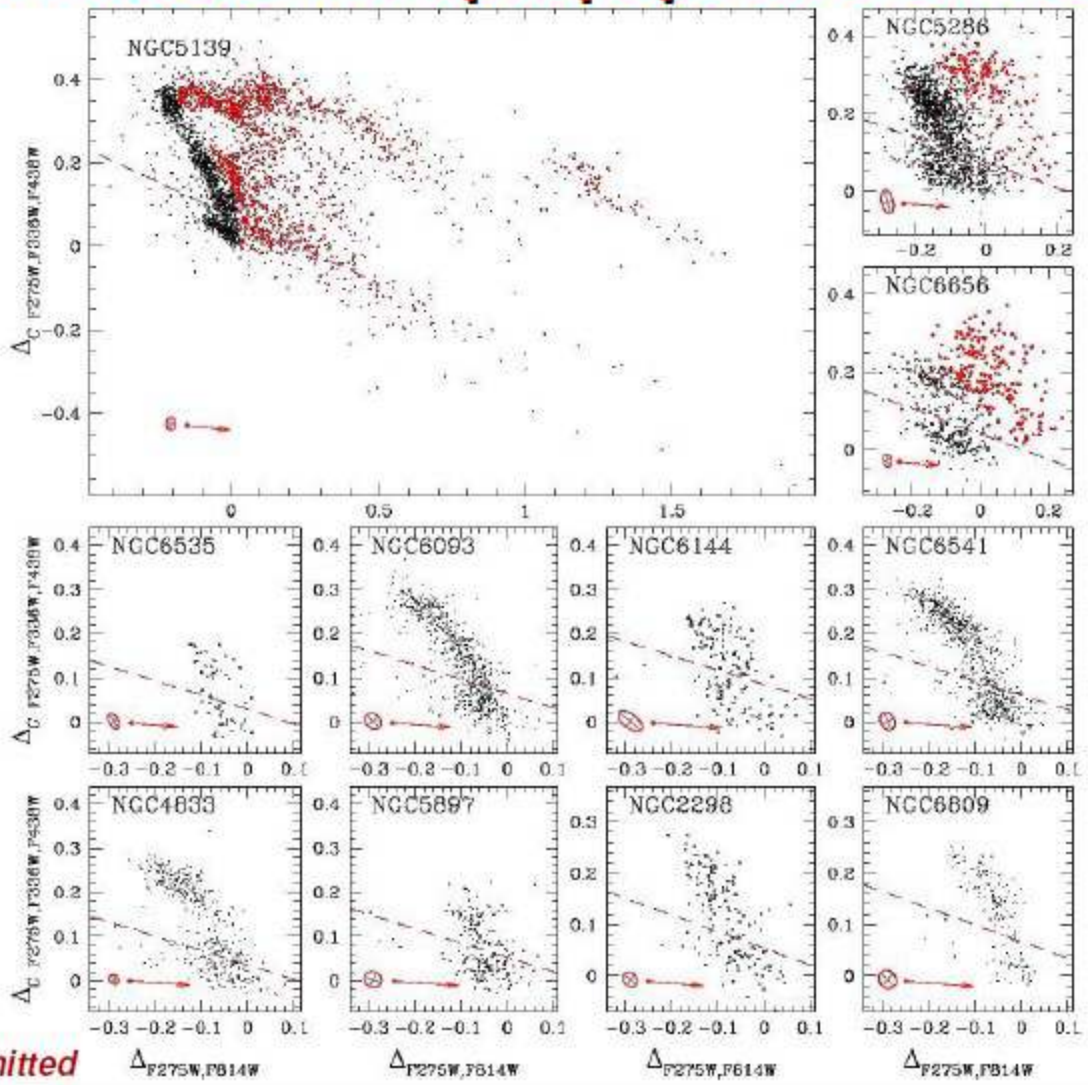

Milone et al. submitted

Reading the Chromosome Map

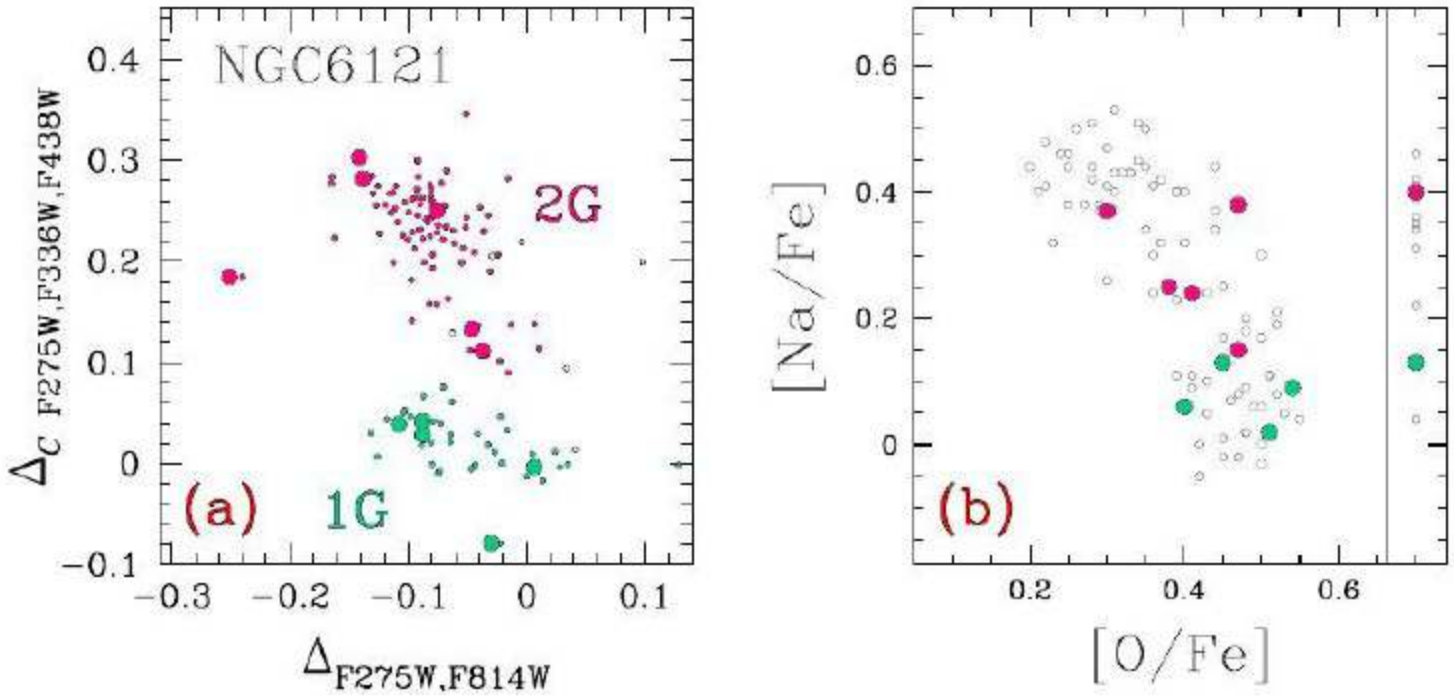

1G stars have primordial composition (Na-poor and O-rich), whereas 2G stars are enhanced in Na and depleted in O

Spectroscopy from:
Marino et al. 2008, A&A, 490, 625

Relations with the main parameters of the host GCs.

1) The RGB width

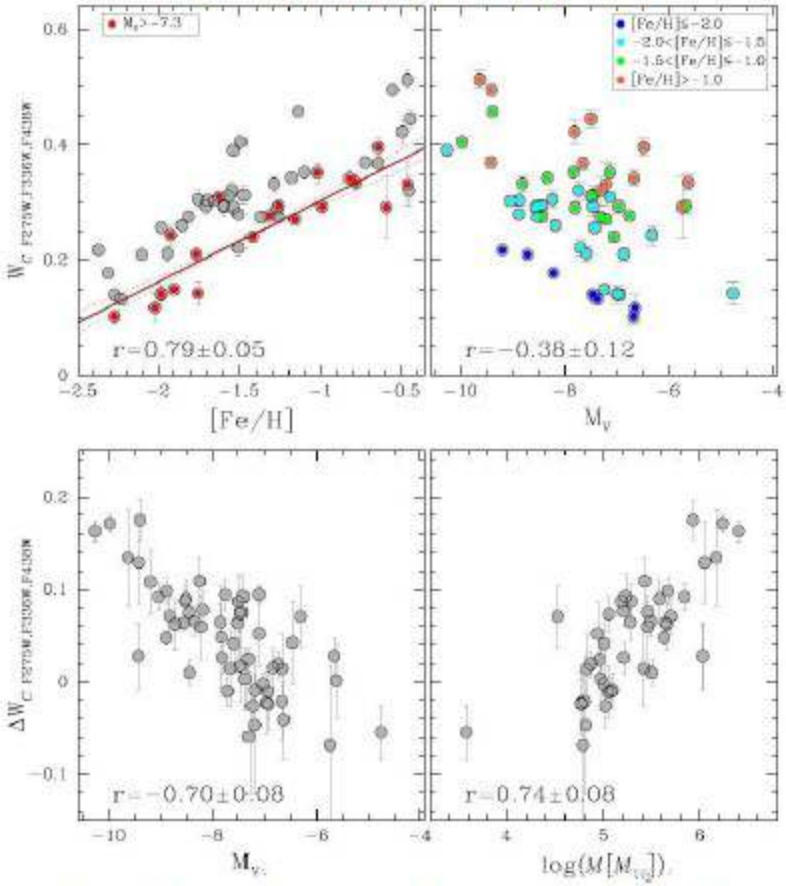

After removing the dependence with the metallicty,
The RGB width correlates with the cluster mass

Relations with the main parameters of the host GCs.

2) The fraction of 1G stars

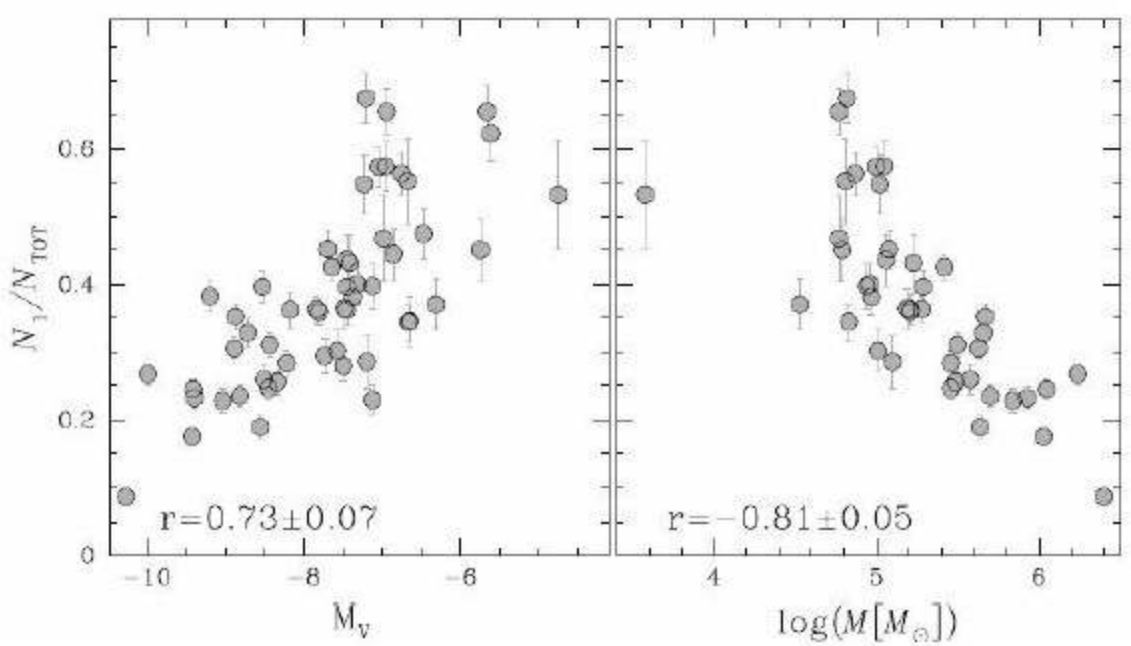

The fraction of 1G stars anti-correlates with the cluster mass.

Relations with the main parameters of the host GCs.

3) The helium variation

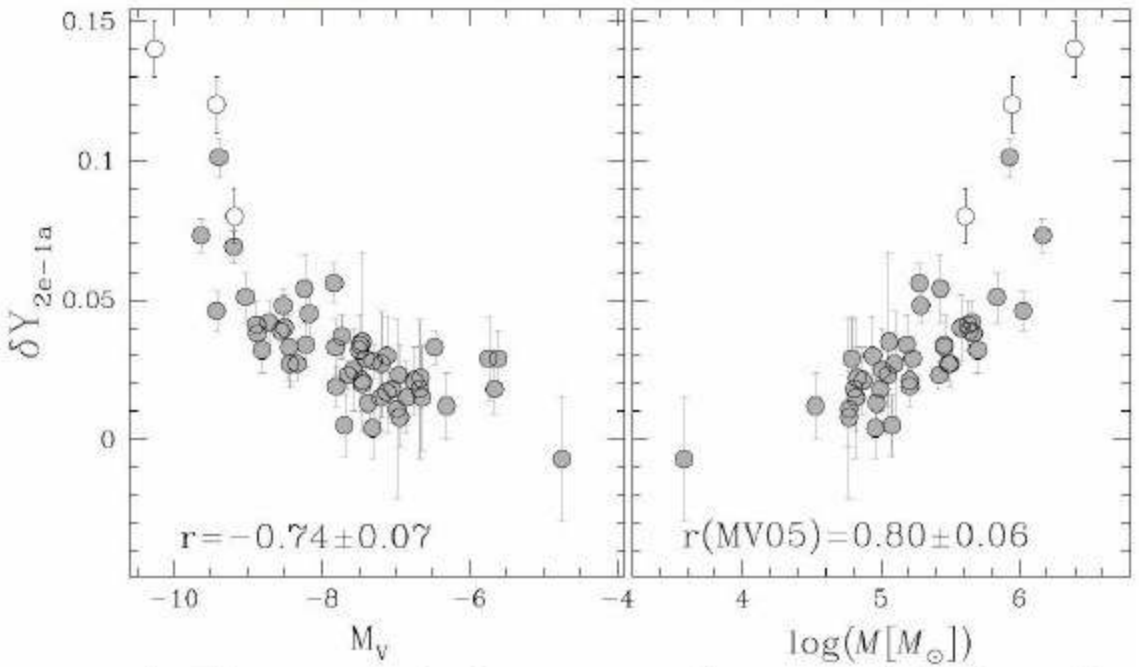

The maximum helium variation correlates with the cluster mass.

The incidence and the complexity of multiple populations both increase with cluster mass

Two classes of Globular Clusters

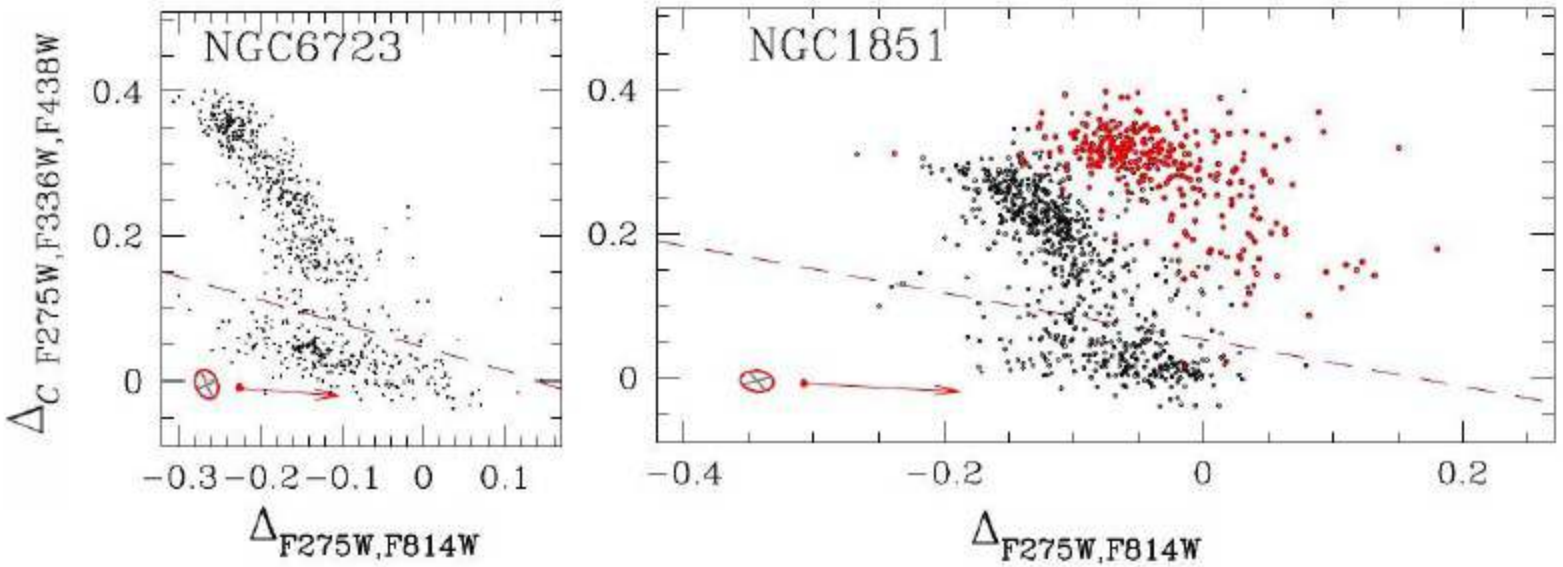

Type I
'normal GCs'
~82%

Type II
'anomalous GCs'
~18%

Anomalous GCs have
1) A distinctive chromosome map

Anomalous GCs: a new class of stellar systems

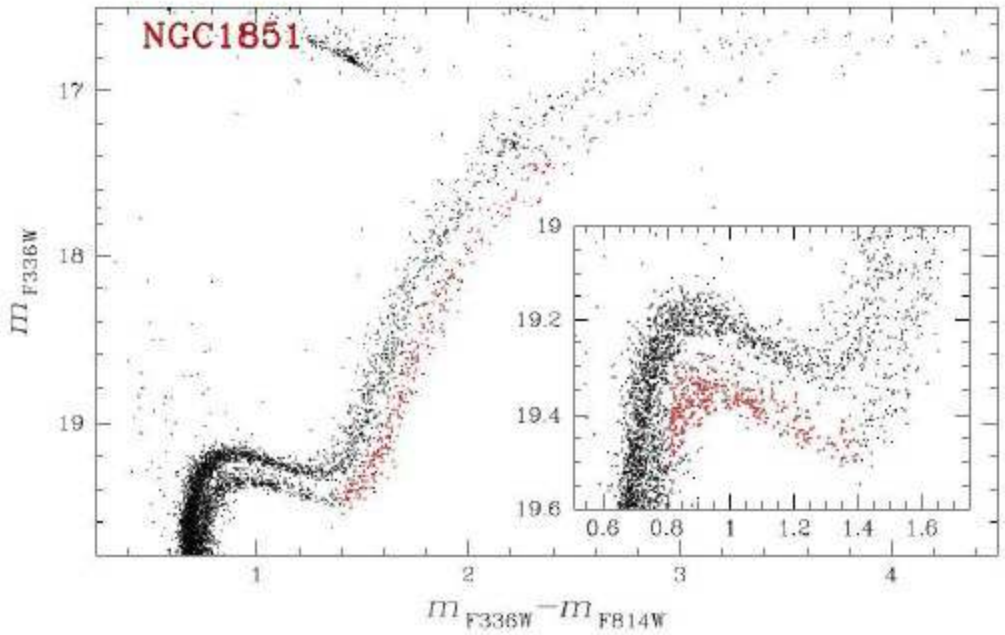

Milone et al. 2008, ApJ, 673, 241

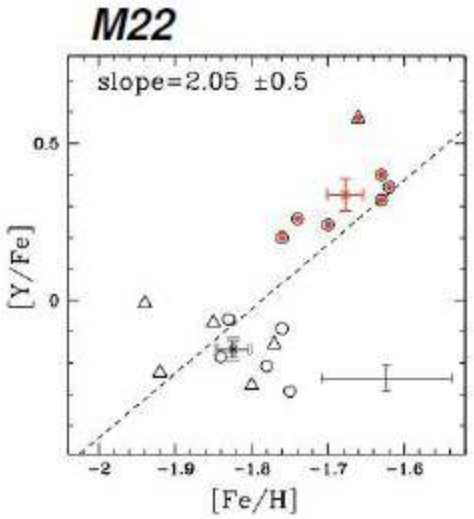

Marino et al. 2009, A&A, 505, 1029

Anomalous GCs have:

1) A distinctive chromosome map;
2) Split SGB in visual filters;
3) Variation in heavy elements and C+N+O.

See also:

Marino et al. 2011ab, 2012, 2105
Carretta et al. 2011ab
Yong et al. 2014
Johnson et al. 2010, 2015
Da Costa et al. 2009
Alves Brito et al. 2013

THE RADIAL DISTRIBUTIONS OF THE TWO MAIN-SEQUENCE COMPONENTS IN THE YOUNG MASSIVE STAR CLUSTER NGC 1856

CHENGYUAN LI[1], RICHARD DE GRIJS[2,3], LICAI DENG[4], ANTONINO P. MILONE[5]
[1]Department of Physics and Astronomy, Macquarie University, Sydney, NSW 2109, Australia

arXiv:1611.04659

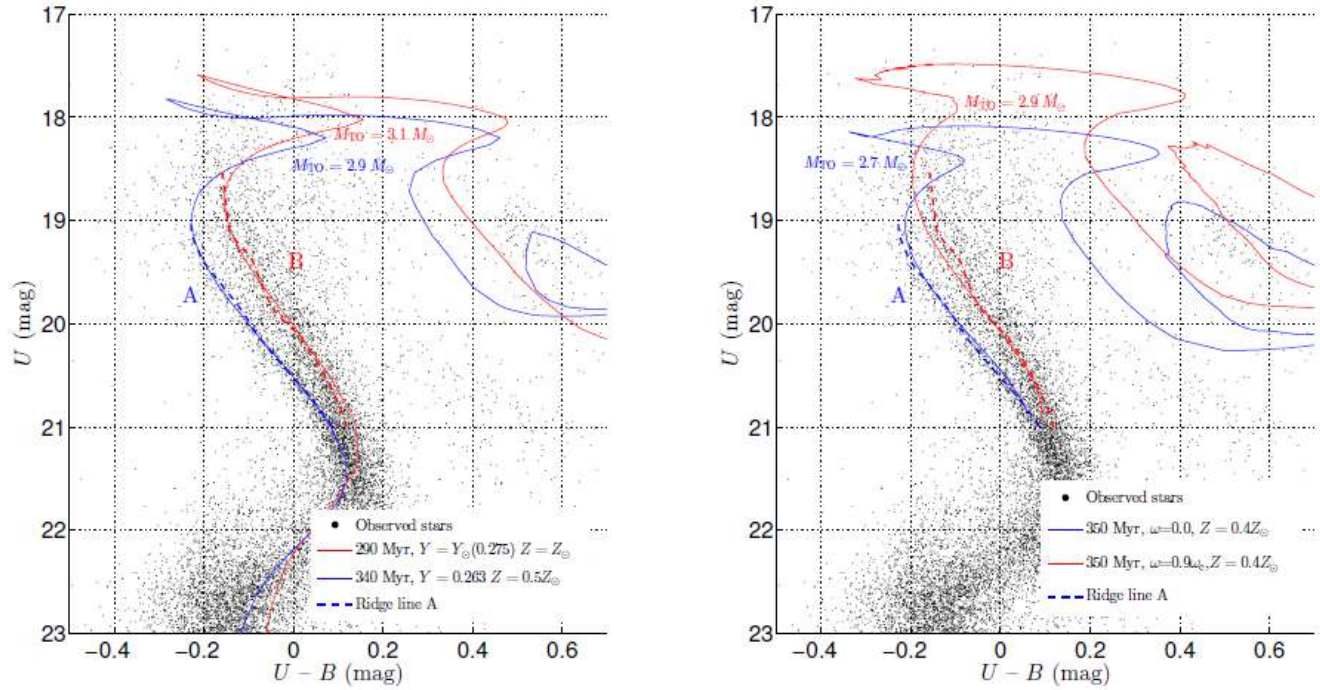

Figure 6. Isochrone fits to the two different MS components in NGC 1856. (left) Bressan et al. (2012) isochrones with different ages, helium abundances and metallicities, as indicated. (right) Both isochrones have the same age and metallicity, but they are characterized by different rotation rates (blue, red solid lines: non-rotating, rapidly rotating stars with $\omega = 0.9\omega_c$. These isochrones were calculated using the Geneva code (Ekström et al. 2012). The blue and red dashed lines are the ridge lines for both MS sequences. We have included the stellar masses of the turn-off (TO) stars in both panels. All stars studied in this paper are B- and early F-type stars.

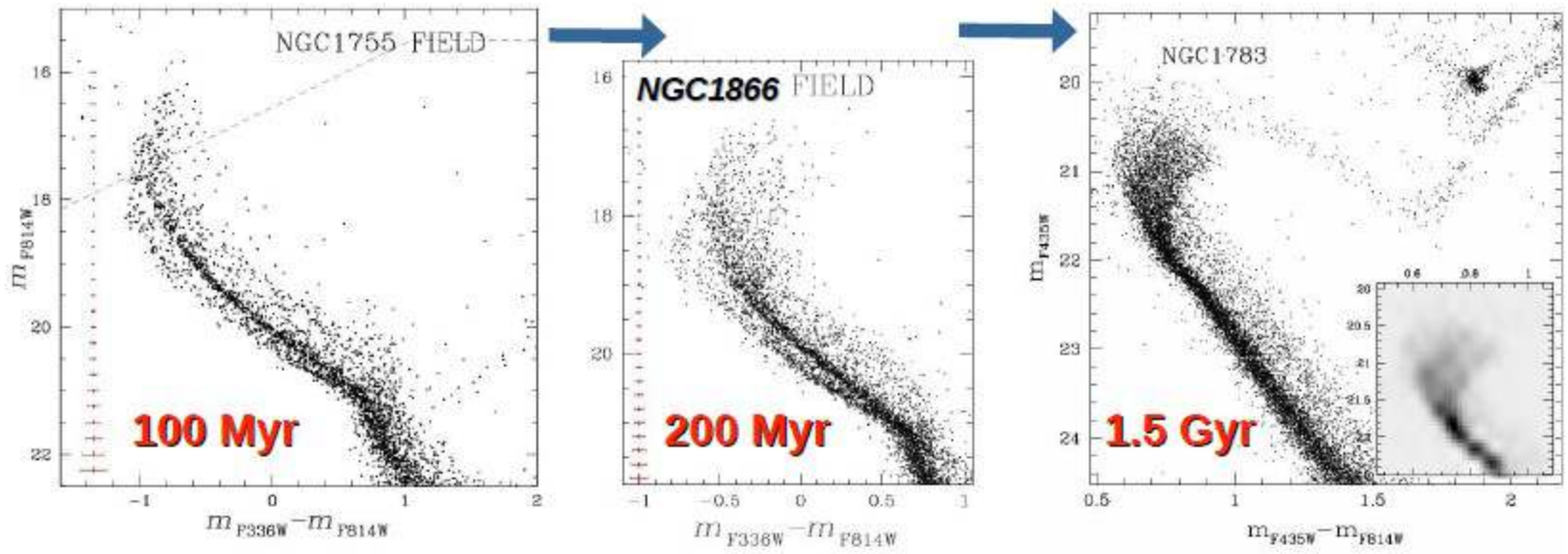

- Young LMC clusters exhibit split MS and eMSTO.
- Rotation is the main responsible for the split MS and the eMSTO.
- Rotation alone seems not able to entirely reproduce the observations.

Summary: U.V.A

– The '**chromosome map**' is a new and powerful tool to identify multiple stellar populations in Galactic GCs. We present the **first atlas of multiple populations** based on multi-wavelength HST photometry of 57 GCs.

– **UBIQUITY.** All the GCs host two distinct groups of 1G stars (with primordial chemical composition) and 2G stars (enhanced in He/N/Na and depleted in C/O).

– **VARIETY.** The RGB width, the fraction of 1G stars, and the helium variation dramatically change from one cluster to another and correlate with the GC mass: **Incidence and complexity of multiple populations both increase with GC mass.**

– **ANOMALOUS GCs** are a new class of stellar systems with heavy-element variations and distinctive feature in the chromosome map. They comprise ~20% of the analysed GCs including Omega Centauri and the Sagittarius nuclear cluster M54.

– **Young GCs** exhibit split MS and eMSTO. Multiple stellar with extreme rotation rates are the main responsible for the unique morphology of their CMDs.